Supporting Information

Synthesis and evaluation of anticancer activity of novel andrographolide derivatives

Ponnam Devendar,[a] Vadithe Lakshma Nayak,[b] Dharmendra Kumar Yadav,[c] Arigari Niranjana Kumar,[a] Jonnala Kotesh Kumar,*[a] KVN Satya Srinivas,*[a] Balasubramanian Sridhar,[d] Feroz Khan,[c] Kakaraparthi Pandu Sastry[a] and Sistla Ramakrishna[c]

[a]*Natural Product Chemistry, CSIR-Central Institute of Medicinal and Aromatic Plants- Research Centre, Boduppal, Hyderabad-500092, India*
[b]*Medicinal Chemistry & Pharmacology, CSIR-Indian Institute of Chemical Technology,Uppal Road, Hyderabad-500007, AP, India*
[c]*Metabolic and Structural Biology Department, CSIR-Central Institute of Medicinal and Aromatic Plants, Lucknow-226015, UP, India*
[d]*Centre for X-ray Crystallography, CSIR-Indian Institute of Chemical Technology,Uppal Road, Hyderabad-500007, AP, India*

**Corresponding Author: Tel: +91-40-27201131 Email:* koteshkumarj@yahoo.com; kvnssrinvas@yahoo.co.in

Instrumentation and chemicals

All non aqueous reactions were carried out under N_2 atmosphere in flame-dried glassware. All reagents were procured from Sigma Aldrich and were used as received. Dichloromethane was freshly distilled from CaH_2. Reactions were monitored by TLC using Kieselgel 60 F_{254} (E. Merck) silica plates and visualised by UV detection (at 254 nm) and staining with 5 % sulphuric acid in methanol. Melting points were measured using A. KRUSS OPTRONIC and are uncorrected. NMR spectra were recorded on Bruker Avance 300/400 MHz in $CDCl_3$ and DMSO-d_6 using TMS as internal standard. IR data are given only for compounds with significant functions (OH, C=O) and were recorded as neat or KBr plate and are reported in wave number (cm^{-1}).

Synthesis and characterization of compounds

General experimental procedure for compounds 3-8 (Scheme 1): Andrographolide **1** (100 mg, 0.28 mmol) and alcohol (1.428 mmol) were taken in acetonitrile (10 mL). To this solution, CAN (313 mg, 0.57 mmol) in minimum amount of acetonitrile was added slowly using dropping funnel. The reaction mixture was stirred at room temperature for 24 h then concentrated to half volume and aquified with 15 ml of water and then extracted with ethyl acetate (3 × 20 ml). The separated organic layers were combined, washed with brine solution, dried over Na_2SO_4 and evaporated under reduced pressure to get crude residue. The residue was purified through silica gel (100-200 mesh) column chromatography (ethyl acetate-petroleum ether) to afford the desired products **3**/**4**/**5**/**6**/**7**/**8**.

3,19-O-ethylideneandrographolide (3) Yield: 96 mg (90%), white solid, m.p. 198–200 °C; IR (KBr): 3412, 2941, 1744, 1673, 1403, 1108 cm^{-1}; ^1H NMR (300 MHz, $CDCl_3$): δ (ppm) 6.92 (t, *J* = 6.3 Hz, 1H), 4.97 (m, 2H), 4.88 (s, 1H), 4.59 (s, 1H), 4.44 (dd, *J* = 10.5 Hz, 6.3 Hz, 1H), 4.23 (d, *J* = 10.5 Hz, 1H), 4.03 (d, *J* = 11.1 Hz, 1H), 3.47–3.38 (m, 2H), 2.83 (br s, 1H), 2.56–2.48 (m, 2H), 2.41–2.0 (m, 3H), 1.81 (m, 3H), 1.69–1.66 (m, 1H), 1.35 (s, 3H), 1.27–1.06 (br m, 6H), 0.85 (s, 3H); ^{13}C NMR (75 MHz, $CDCl_3$): δ (ppm) 170.18, 148.90, 146.51, 127.99, 109.12, 92.19, 80.0, 74.42, 68.90, 66.09, 55.70, 54.58, 38.79, 37.54, 36.65, 36.02, 25.94, 24.70, 22.71, 21.77, 21.23, 15.22; ESI-MS: positive ion mode: *m/z* 399.41 $[M+Na]^+$, observed for $C_{22}H_{32}O_5$.

3,19-O-*n*-propylideneandrographolide (4) Yield: 84 mg (76%), yellow solid, m.p. 176–178 °C; IR (KBr): 3403, 2937, 1726, 1674, 1401, 1102 cm^{-1}; ^1H NMR (300 MHz,

$CDCl_3$): δ (ppm) 6.97 (t, *J* = 6.9 Hz, 1H), 5.03 (d, *J* = 5.4 Hz, 1H), 4.90 (s, 1H), 4.74 (t, *J* = 4.8 Hz, 1H), 4.60 (s, 1H), 4.46 (dd, *J* = 10.5 Hz, 6.3 Hz, 1H), 4.26 (dd, *J* = 10.5 Hz, 1.8 Hz, 1H), 4.03 (d, *J* = 11.1 Hz, 1H), 3.51–3.42 (m, 2H), 2.58–2.52 (m, 2H), 2.43–1.16 (br m, 12H), 1.36 (s, 3H), 0.92 (t, *J* = 7.5 Hz, 3H), 0.81 (s, 3H); ESI-MS: positive ion mode: *m/z* 391.07 $[M+H]^+$, observed for $C_{23}H_{34}O_5$.

3,19-O-*n*-butylideneandrographolide (5) Yield: 86 mg (75%), light yellow solid, m.p. 132–134 °C; δ (ppm) 6.95 (t, *J* = 6.6 Hz, 1H), 5.03 (d, *J* = 6 Hz, 1H), 4.89 (s, 1H), 4.80 (t, *J* = 4.8 Hz, 1 H), 4.60 (s, 1H), 4.46 (dd, *J* = 10.5 Hz, 6.3 Hz, 1H), 4.26 (dd, *J* = 10.5 Hz, 2.1 Hz, 1H), 4.03 (d, *J* = 11.4 Hz, 1H), 3.51–3.41 (m, 2H), 2.63–1.16 (br m, 16H) 1.36 (s, 3H), 0.91 (m, 3H), 0.81 (s, 3H); ESI-MS: positive ion mode: *m/z* 405.34 $[M+H]^+$, 427.40 $[M+Na]^+$, observed for $C_{24}H_{36}O_5$.

3,19-O-*n*-pentylideneandrographolide (6) Yield: 72 mg (61%), yellow solid, m.p. 162–164 °C; ^{1}H NMR (300 MHz, $CDCl_3$): δ (ppm) 6.94 (t, *J* = 6.9 Hz, 1H), 5.02 (d, *J* = 5.1 Hz, 1H), 4.89 (s, 1H), 4.84 (t, *J* = 5.1 Hz, 1H), 4.61 (s, 1H), 4.45 (dd, *J* = 10.5 Hz, 6.1 Hz, 1H), 4.26 (d, *J* = 10.5 Hz, 1H), 4.03 (d, *J* = 11.4 Hz, 1H), 3.41–3.51 (m, 2H), 2.56–2.27 (m, 4H), 2.04–0.90 (br m, 17H), 1.36 (s, 3H), 0.81 (s, 3H); ESI-MS: positive ion mode: *m*/*z* = 440.94 $[M+Na]^+$, observed for $C_{25}H_{38}O_5$.

3,19-O-*n*-hexylideneandrographolide (7) Yield: 43 mg (35 %), white solid, m.p. 181–183 °C; IR (KBr): 3411, 2940, 1744, 1674, 1400, 1081 cm^{-1}; ^{1}H NMR (300 MHz, $CDCl_3$): δ (ppm) 6.96 (t, *J* = 6.9 Hz, 1H), 5.03 (d, *J* = 5.1 Hz, 1H), 4.90 (s, 1H), 4.79 (t, *J* = 4.8 Hz, 1H), 4.60 (s, 1H), 4.46 (dd, *J* = 10.5 Hz, 6.3 Hz, 1H), 4.26 (dd, *J* = 10.5 Hz, 2.1 Hz, 1H), 4.03 (d, *J* = 11.1 Hz, 1H), 3.49–3.41 (m, 2H), 2.57–2.52 (m, 2H), 2.45–0.90 (br m, 21H), 1.36 (s, 3H), 0.81 (s, 3H); ^{13}C NMR (75

MHz, $CDCl_3$): δ (ppm) 170.17, 148.91, 146.60, 128.04, 109.14, 95.31, 79.94, 74.43, 68.99, 66.15, 55.77, 54.76, 38.85, 37.61, 36.94, 36.08, 35.17, 31.77, 25.99, 24.75, 23.60, 22.76, 22.61, 21.79, 15.28, 14.04; ESI-MS: positive ion mode: *m*/*z* = 433.40 $[M+H]^+$, 455.38 $[M+Na]^+$, observed for $C_{26}H_{40}O_5$.

3,19-O-benzylideneandrographolide (8)

Yield: 111 mg (86 %), yellow solid, m.p. 142–144 °C; ^1H NMR (300 MHz, $CDCl_3$): δ (ppm) 7.34–7.50 (m, 5H), 6.94 (t, *J* = 6.0 Hz, 1H), 5.76 (s, 1H), 5.02 (d, *J* = 3.9 Hz, 1H), 4.91 (s, 1H), 4.63 (s, 1H), 4.42 (dd, *J* = 10.5 Hz, 6.3 Hz, 1H), 4.26–4.19 (m, 2H), 3.67 (dd, *J* = 12.6 Hz, 4.5 Hz, 1H), 3.59 (d, *J* = 11.4 Hz, 1H), 2.75 (s, 1H), 2.58–2.53 (m, 2H), 2.50–2.37 (m, 2H), 2.06–2.04 (m, 1H), 1.98–1.78 (br m, 4H), 1.49 (s, 3H), 1.34–1.21 (br m, 3H), 0.87 (s, 3H); ESI-MS: positive ion mode: *m*/*z* = 439.16 $[M+H]^+$, 461.08 $[M+Na]^+$, observed for $C_{27}H_{34}O_5$.

Experimental procedure and characterization for 14-acetyl-3,19-O-ethylideneandrographolide (3a): Compound **3** (100 mg, 0.2659 mmol) and TEA (0.5 mL) and acetic anhydride (1 mL) were taken in to CH_2Cl_2 (10 mL) and stirred at RT for 30 min. The completion of the reaction monitored by TLC, The reaction mixture was concentrated and poured into cold water, then filtered and dried. It was crystallized in CH_2Cl_2:MeOH (9:1) at RT to get desired compound **3a**. Yield: 105 mg (95 %), white crystalline solid, m.p. 150–152 °C; IR (KBr): 3490, 2984, 1754, 1740, 1674, 1403, 1072 cm^{-1}; ^1H NMR (300 MHz, $CDCl_3$): δ (ppm) 6.96 (t, *J* = 6.9 Hz, 1H), 5.89 (d, *J* = 5.4 Hz, 1H,) 4.93 (q, *J* = 4.8 Hz, 1H), 4.84 (s, 1H), 4.53–4.48 (m, 2H), 4.20 (dd, *J* = 11.1 Hz, 1.5 Hz, 1H), 3.99 (d, *J* = 11.4 Hz, 1H), 3.45–3.35 (m, 2H), 2.41–2.36 (m, 2H), 2.24–1.12 (br m, 12H), 2.08 (s, 3H), 1.33

(s, 3H), 0.74 (s, 3H); ^{13}C NMR (300 MHz, $CDCl_3$): δ (ppm) 170.84, 169.36, 150.65, 147.11, 124.34, 109.36, 92.58, 80.35, 71.93, 69.28, 68.16, 56.02, 55.10, 39.16, 37.93, 37.06, 36.42, 26.35, 25.62, 23.09, 22.18, 21.66, 21.08, 15.22; ESI-MS: positive ion mode: m/z = 419 $[M+H]^+$, 441 $[M+Na]^+$, 859 $[2M+Na]^+$, observed for $C_{24}H_{34}O_6$. **Crystal data for compound 3a:** $C_{24}H_{34}O_6$, M = 418.51, colourless needle, 0.15 × 0.08 × 0.06 mm^3, orthorhombic, space group $P2_12_12_1$ (No. 19), a = 11.987(3), b = 12.551(3), c = 14.454(4) Å, V = 2174.7(9) Å^3, Z = 4, D_c = 1.278 g/cm^3, F_{000} = 904, CCD Area Detector, MoKα radiation, λ = 0.71073 Å, T = 294(2)K, $2\theta_{max}$ = 50.0º, 21307 reflections collected, 2185 unique (R_{int} = 0.0341). Final *GooF* = 1.123, *R1* = 0.0450, *wR2* = 0.1114, *R* indices based on 1977 reflections with I>2σ(I) (refinement on F^2), 275 parameters, 0 restraints, μ = 0.091 mm^{-1}. CCDC 937572 contains supplementary crystallographic data for the structure.

Experimental procedure and characterization of 14-deoxy-11,12-didehydro-3,19-O-ethylidene andrographolide (3b): Compound **3** (100 mg, 0.26 mmol) was dissolved in anhydrous pyridine (2 mL), and then activated alumina (0.2 g) was added and it was stirred at 100–110 °C for 12 h. The completion of the reaction monitored by TLC, it was cooled and filtered, washed with CH_2Cl_2 (3 × 10 mL), and evaporated to obtain a residue. It was crystallized from 2-propanol:water (1:4) to yield compound **3b**. Yield: 85.6 mg (90%), white solid, m.p. 120–122 °C; IR (KBr): 2936, 1758, 1624, 1451, 1086 cm^{-1}; ^{1}H NMR (300 MHz, $CDCl_3$): δ (ppm) 7.16 (s, 1H), 6.91 (dd, J = 10.2 Hz, 15.6 Hz, 1H), 6.12 (d, J = 15.9 Hz, 1H), 4.97 (q, J = 4.5 Hz, 1H), 4.85–4.79 (m, 3H), 4.55 (s, 1H), 4.09 (d, J = 10.8 Hz, 1H),

3.50–3.40 (m, 2H), 2.51–1.10 (br m, 13H), 1.38 (s, 3H), 0.93 (s, 3H); ^{13}C NMR (75 MHz, $CDCl_3$): δ 172.68, 148.37, 143.55, 136.23, 129.60, 121.68, 109.88, 92.69, 80.89, 70.03, 69.43, 61.95, 54.52, 38.92, 37.79, 37.19, 36.75, 26.30, 22.39, 22.13, 21.64, 16.42; ESI-MS: positive ion mode: *m*/*z* = 381.29 $[M+Na]^+$, observed for $C_{22}H_{30}O_4$.

Experimental procedure and characterization for 14-deoxy-14,15-dehydro-3,19-O-ethylidene andrographolide (3c): Compound **3a** (100 mg, 0.239 mmol) and DMAP (0.25 mmol) were taken into CH_2Cl_2 (5 mL) and stirred at RT. After completion of reaction (1 h, TLC monitoring), diluted with water (20 ml) and extracted with CH_2Cl_2 (2 × 20 mL). The combined organic layers were washed with water (5 mL), brine solution (5 mL), dried over Na_2SO_4 and evaporated under reduced pressure. The residue was purified through silica gel (100-200 mesh) column chromatography (in ethyl acetate-petroleum ether) to afford the desired product **3c**. Yield: 76 mg (72 %), light yellow solid, m.p. 208-210 °C; IR (KBr): 3435, 2936, 1767, 1649, 1442, 1040 cm^{-1}; ^{1}H NMR (300 MHz, $CDCl_3$): δ (ppm) 6.99 (s, 1H), 6.69 (t, *J* = 6.6 Hz, 1H), 6.15 (d, *J* = 3.0 Hz, 1H), 4.98–4.95 (m, 2H), 4.43 (s, 1H), 4.06–4.02 (d, *J* = 12.0 Hz, 1H), 3.51–3.39 (m, 2H), 2.52–1.19 (br m, 15H), 1.37 (s, 3H), 0.81 (s, 3H); ^{13}C NMR ($CDCl_3$, 75 MHz): δ (ppm) 168.29, 147.11, 145.85, 144.48, 126.20, 109.35, 105.35, 92.63, 80.41, 69.34, 56.25, 55.13, 39.33, 37.98, 37.11, 36.54, 30.08, 26.40, 26.37, 23.13, 22.23, 21.67, 15.72; ESI-MS: positive ion: *m/z* 381.29 $[M+Na]^+$, observed for $C_{22}H_{30}O_4$.

General experimental procedure and characterization for Compound 3d, 3e, and 3f: Compounds **3**/**3a**/**3b** (0.2659 mmol) and *m*CPBA (0.39 mmol) in CH_2Cl_2

(10 mL) were stirred for 4 h. After completion of the reaction (TLC monitoring), the mixture was washed with aq. Na_2CO_3, brine and water successively. The CH_2Cl_2 phase was dried over Na_2SO_4, filtered and concentrated. The concentrated residue was purified over silica gel (100-200 mesh) column chromatography (in ethyl acetate-petroleum ether) to afford the desired products **3d**/**3e**/**3f**.

8,17-epoxy-3,19-O-ethylideneandrographolide (3d) Yield: 74 mg (68 %), white solid, m.p. 138–140 °C; IR (KBr): 3423, 2944, 1753, 1674, 1403, 1108 cm^{-1}; ^1H NMR (300 MHz, $CDCl_3$): δ (ppm) 6.79 (t, *J* = 5.7 Hz, 1H), 4.98 (m, 2H), 4.38 (dd, *J* = 10.2 Hz, 6.0 Hz, 1H), 4.24 (d, *J* = 10.2 Hz, 1H), 4.03 (d, *J* = 11.1 Hz, 1H), 3.48–3.43 (m, 2H), 2.87 (s, 1H), 2.87–2.65 (m, 2H) 2.29–1.18 (br m, 14H), 1.39 (s, 3H), 0.94 (s, 3H); ^{13}C NMR (300 MHz, $CDCl_3$): δ (ppm) 170.52, 146.49, 129.47, 92.68, 80.06, 74.09, 69.10, 65.64, 60.41, 54.59, 53.72, 51.49, 40.05, 36.89, 36.33, 36.16, 26.31, 23.02, 21.63, 21.39, 20.86, 15.8; ESI-MS: positive ion mode: *m*/*z* 415.19 $[M+H]^+$, observed for $C_{22}H_{32}O_6$.

14-acetyl-8,17-epoxy-3,19-O-ethylideneandrographolide (3e) Yield: 80 mg (70 %), yellow solid, m.p.: 121-123 °C; IR (KBr): 3463, 2949, 1753, 1740, 1674, 1404, 1105 cm^{-1}; ^1H NMR (400 MHz, DMSO-d_6): δ (ppm) 6.93 (t, *J* = 6.8 Hz, 1H), 5.83 (d, *J* = 6 Hz, 1H), 4.99 (q, *J* = 4.4 Hz, 1H), 4.55 (dd, *J* = 10.8 Hz, 6 Hz, 1H), 4.23 (dd, *J* = 11.2 Hz, 1.2 Hz, 1H) 3.98 (d, *J* = 11.2 Hz, 1H), 3.39 (m, 2H), 2.67 (d, *J* = 3.2 Hz, 1H), 2.30–2.26 (m, 1H), 2.16–2.12 (m, 1H), 2.05 (s, 3H), 1.88–1.86 (m, 1H), 1.79–1.74 (m, 3H), 1.66–1.63 (d, *J* = 13.2 Hz, 1H), 1.48–1.44 (m, 1H), 1.33–1.30 (m, 2H), 1.25 (s, 3H), 1.21–1.11 (m, 6H), 0.88 (s, 3H); ^{13}C NMR (125 MHz, DMSO-d_6); δ (ppm) 170.11, 168.95, 150.53, 123.04, 91.39,

78.87, 71.32, 67.69, 58.18, 53.03, 52.87, 49.39, 39.5, 35.94, 35.41, 35.30, 25.53, 22.54, 21.19, 20.97, 20.64, 20.01, 14.66; ESI-MS**:** positive ion mode: *m/z* 457.19 $[M+Na]^+$, observed for $C_{24}H_{34}O_7$. **Crystal data for compound 3e:** $C_{24}H_{34}O_7$, M = 434.51, colorless plate, 0.18 × 0.17 × 0.09 mm^3, orthorhombic, space group $P2_12_12_1$ (No. 19), a = 12.4798(16), b = 12.7207(17), c = 14.3452(19) Å, V = 2277.3(5) $Å^3$, Z = 4, D_c = 1.267 g/cm^3, F_{000} = 936, CCD Area Detector, MoKα radiation, λ = 0.71073 Å, T = 294(2)K, $2\theta_{max}$ = 50.0º, 21934 reflections collected, 2280 unique (R_{int} = 0.0219). Final *GooF* = 1.053, *R1* = 0.0339, *wR2* = 0.0931, *R* indices based on 2171 reflections with I>2σ(I) (refinement on F^2), 285 parameters, 0 restraints, μ = 0.092 mm^{-1}. CCDC 943354 contains supplementary Crystallographic data for the structure.

14-deoxy-11,12-didehydro-8,17-epoxy-3,19-O-ethylideneandrographolide (3f) Yield: 64 mg (65 %) light yellow solid, m.p. 79–81 °C; IR (KBr): 3451, 2942, 1753, 1403, 1097 cm^{-1}; ^1H NMR ($CDCl_3$, 300 MHz): δ (ppm) 7.14 (s, 1H), 6.56 (dd, J = 9.0 Hz, 3.0 Hz, 1H), 4.98–4.78 (m, 3H), 4.11 (m, 1H), 3.45 (m, 2H), 2.79 (s, 1H), 2.54 (d, J = 3.0 Hz, 1H), 2.28–0.94 (br m, 14H) 1.38 (s, 3H), 0.91 (s, 3H); ^{13}C NMR ($CDCl_3$, 300 MHz): δ (ppm) 172.47, 144.49, 131.20, 129.07, 124.53, 92.70, 80.62, 69.94, 69.31, 59.45, 58.40, 54.15, 51.51, 39.24, 37.48, 37.05, 35.75, 26.35, 21.64, 21.55, 20.79, 16.46; ESI-MS: positive ion mode: *m/z* 375.40 $[M+H]^+$, observed for $C_{22}H_{30}O_5$.

Cytotoxicity evaluation

The cytotoxicity of the compounds was determined using MTT assay. 1×10^6 cells/well were seeded in 200 µl DMEM, supplemented with 10 % FBS in each well of

96-well micro culture plates and incubated for 24 h at 37 ^{0}C in a CO_2 incubator. Compounds, diluted to the desired concentrations in culture medium, were added to the wells with respective vehicle control. After 48 h of incubation, 10 µl MTT (3-(4,5-dimethylthiazol-2-yl)-2,5-diphenyl tetrazolium bromide) (5 mg/ml) was added to each well and the plates were further incubated for 4 h. Then the supernatant from each well was carefully removed, formazon crystals were dissolved in 100 µl of DMSO and absorbance at 540 nm wavelength was recorded.

Molecular modeling parameters and energy minimization

To find the possible interactions of compound **1** with anticancer target, we docked all compounds at target protein αβ-tubulin for HeLa cell and epidermal growth factor receptor (EGFR) for human lung cancer. Sybyl X 2.0 interfaced with Surflex-Dock module was used for molecular docking. Program automatically docks ligand into binding pocket of a target protein by using protomol based algorithm and empirically produced scoring function. The X-ray crystallographic structures of αβ-tubulin complex with ligand (PDB: 1JFF) and EGFR (PDB: 2ITW) was taken from the protein data bank (PDB) and modified for docking calculations. Since there are no PDB ID available in protein data bank (www.rcsb.org) of these target i.e. ACHN (renal cell carcinoma), B-16 (melanoma) and IEC-6 (small intestine) we are not perform docking study. Co-crystallized ligand was removed from the structure, water molecules were removed, H atoms were added and side chains were fixed during protein preparation. Protein structure minimization was performed by applying Tripos force field and partial atomic charges were calculated by Gasteiger-Huckel method. In reasonable binding pocket, all the compounds were docked into the binding pocket and 20 possible active docking

conformations with different scores were obtained for each compound. During the docking process, all of the other parameters were assigned their default values.[1-3]

X-ray method

X-ray data of compound **3a** and **3e** were collected at room temperature using a Bruker Smart Apex CCD diffractometer with graphite monochromated MoKα radiation (λ = 0.71073 Å) with ω-scan method.[4] Preliminary lattice parameters and orientation matrices were obtained from four sets of frames. Unit cell dimensions were determined using 5607 reflections for compound **3a** and 5435 reflections for compound **3e**. Integration and scaling of intensity data were accomplished using SAINT program.[4] The structures were solved by Direct Methods using SHELXS97[5] and refinement was carried out by full-matrix least-squares technique using SHELXL97.[5] Anisotropic displacement parameters were included for all non-hydrogen atoms. All H atoms were positioned geometrically and treated as riding on their parent C atoms, with C-H distances of 0.93--0.96 Å, and with $U_{iso}(H) = 1.2U_{eq}$ (C) or $1.5U_{eq}$ for methyl atoms. In the absence of significant anomalous scattering efforts, Friedel pairs were merged. The absolute configuration of the procured material was known in advance.

Suppl. Table 2. Comparison of binding affinity of **3**, **3a**, **3d**, **3e**, **7** and the standard drug doxorubicin against anticancer target EGFR kinase (PDB: 21TW).

Compound	Total Score	Binding site amino acid residues (with in 4Ă)	Amino acid in H-bond	Length of H-bond (Å)	No. of H-bonds
3	5.3004	LEU-718, GLY-719, PHE-723, VAL-726, ALA-743, LYS-745, GLU-762, MET-766, CYS-775, LEU-788, THR-790, GLN-791, LEU-792, MET-793, ARG-841, ASN-842, LEU-844, THR-854, ASP-855	THR-854 ASP-855	1.9 1.9	2
3a	5.7828	LEU-718, GLY-719, PHE-723, VAL-726, LYS-728, ALA-743, LYS-745, THR-790, LEU-792, MET-793, PRO-794, GLY-796, CYS-797, ASN-842, LEU-844, LYS-852, THR-854, ASP-855	THR-854	2.1	1
3d	5.0596	LEU-718, GLY-719, VAL-726, ALA-743, LYS-745, MET-766, CYS-775, LEU-788, THR-790, LEU-792, MET-793, PRO-794, GLY-796, CYS-797, LEU-844, THR-854, ASP-855	THR-854 THR-790 MET-793	1.9 1.9 2.1	3
3e	4.7946	ARG-2, LEU-248, ASN-249, ALA-250, ASP-251, LYS-254, ASP-329, LYS-352, GLY-10, GLN-11, ALA-12, GLN-15, ASP-69, GLU-71, ALA-99, ASN-101, SER-140, GLY-142, GLY-143, GLY-144, THR-145, GLY-146, ILE-171, TYR-172, PRO-173, ALA-174, VAL-177, SER-178, THR-179, ALA-180, GLU-183, ASN-206, TYR-224	GLY-144 LYS-254	2.0 1.8	2
7	5.3047	PHE-723, VAL-726, ALA-743, LYS-745, GLU-762, MET-766, CYS-775, LEU-788, THR-790, GLN-791, LEU-792, MET-793, CYS-797, ASP-837, ARG-841, ASN-842, LEU-844, THR-854, ASP-855, ASP-857	-	-	-
Doxorubicin	4.9812	LEU-718, GLY-719, ALA-722, PHE-723, VAL-726, ALA-743, LYS-745, GLU-762, MET-766, CYS-775, LEU-788, THR-790, GLN-791, LEU-792, MET-793, PRO-794, GLY-796, ARG-841, ASN-842, LEU-844, THR-854, ASP-855	ASP-855 THR-854 GLU-762 MET-793	1.8 1.9 1.9 1.8	4

Suppl. Table 3. Comparison of binding affinity of **1**, **3a**, **3e**, **7** and standard drug doxorubicin against anticancer target α,β-tubulin (PDB ID: 1JFE).

Compound	Total Score	Binding site amino acid residues (with in 4Ă)	Amino acid in H-bond	Length of H-bond (Ă)	No. of H-bonds
1	8.9906	LEU-248, ASN-249, LYS-254, LYS-352, GLY-10, GLN-11, ALA-12, ALA-99, ASN-101, SER-140, PHE-141, GLY-142, GLY-143, GLY-144, THR-145, GLY-146, ILE-171, TYR-172, PRO-173, ALA-174, SER-178, THR-179, ALA-180, GLU-183, ASN-206, TYR-224	ALA-174, GLY-142, ILE-171, GLY-146, GLN-11	2.1 1.9 1.9 1.9 1.8	5
3a	4.7654	LEU-248, ASN-249, LYS-254, LYS-352, VAL-9, GLY-10, GLN-11, ALA-12, GLY-13, ASP-69, LEU-70, ALA-99, ASN-101, HIS-139, SER-140, PHE-141, GLY-142, GLY-143, GLY-144, THR-145, GLY-146, ILE-171, TYR-172, PRO-173, ALA-174, SER-178, THR-179, ALA-180, GLU-183, ASN-186, ASN-206, TYR-224	ALA-12, LYS-254 GLY-146	1.8 2.1 2.0	3
3e	4.7946	ARG-2, LEU-248, ASN-249, ALA-250, ASP-251, LYS-254, ASP-329, LYS-352, GLY-10, GLN-11, ALA-12, GLN-15, ASP-69, GLU-71, ALA-99, ASN-101, SER-140, GLY-142, GLY-143, GLY-144, THR-145, GLY-146, ILE-171, TYR-172, PRO-173, ALA-174, VAL-177, SER-178, THR-179, ALA-180, GLU-183, ASN-206, TYR-224	GLY-144 LYS-254	2.0 1.8	2
7	5.2077	LEU-248, ASN-249, LYS-254, ASP-329, LYS-352, GLY-10, GLN-11, ALA-12, GLN-15, ASP-69, LEU-70, GLU-71, VAL-74, ALA-99, ASN-101, SER-140, PHE-141, GLY-142, GLY-143, GLY-144, THR-145, GLY-146, ILE-171, TYR-172, PRO-173, ALA-174, VAL-177, SER-178, THR-179, ALA-180, GLU-183, ASN-206, GLU-207, TYR-210, TYR-224	VAL-177	1.9	1
Doxorubicin	4.6952	LEU-248, ASN-249, ALA-250, GLY-10, GLN-11, ALA-12, GLN-15, ILE-16 ASP-69, LEU-70, GLU-71, VAL-74, ASP--99, ASN-101, SER-140, GLY-142, GLY-143, GLY-144, THR-145, GLY-146, ILE-171, TYR-172, PRO-173, ALA-174, THR-179, ALA-180, GLU-183, ASN-206, TYR-224, LEU-227, ASN-228	ILE-171 SER-140 GLY-142	1.9 1.7 1.8	3

Suppl. Table 4. Compliance of active 3,19-O-acetal derivatives of andrographolide to the computational parameters of pharmacokinetics (ADME).

Compound	log S for aqueous solubility	LogP	log Khsa for Serum Protein Binding	log BB for blood-brain barrier penetration	No. of metabolic reactions	Predicted CNS Activity	log hERG for K+ Channel Blockage	Apparent Caco-2 Permeability (nm/sec)	Apparent MDCK Permeability (nm/sec)	Polar SA (PSA)	log Kp for skin permeability	% Human Oral Absorption in GI (+-20%)
1	-3.049	2.113	-0.208	-1.307	6	-2	-3.609	254.165	112.551	97.854	-3.857	78.516
3	-3.606	2.872	0.022	-0.43	4	-1	-3.449	1421.597	723.575	73.43	-2.7	100
3a	-3.671	3.001	-0.107	-0.272	4	-1	-3.874	2346.394	1243.682	86.463	-2.291	100
3d	-2.533	1.784	-0.401	-0.415	2	-1	-2.99	1333.982	675.495	85.44	-2.813	92.172
3e	-1.83	1.913	-0.73	-0.519	2	-1	-3.107	1041.237	516.796	103.907	-3.021	90.439
7	-5.003	4.629	0.404	-0.753	4	-1	-4.403	1490.726	761.68	74.909	-2.231	100
8	-5.442	4.551	0.554	-0.458	4	-1	-5.033	1373.148	696.958	72.651	-2.139	100
Doxorubicin	-2.775	0.188	-0.543	-3.101	9	-2	-6.268	2.15	0.716	215.962	-7.957	20
Stand. Range*	(-6.5 / 0.5)	-2.0/ 6.5	(-1.5 / 1.5)	(-3.0 / 1.2)	(1 / 8)	–2 (inactive) +2 active)	(concern below -5)	(<25 poor, >500 great)	(<25 poor, >500 great)	(7.0 / 200.0)	(–8.0 to –1.0, Kp in cm/hr)	(<25% is poor)

Footnote: * For 95% of known drugs, based on –Qikprop software (Schrödinger, USA). hERG= Human Ether-a-go-go-Related Gene, Caco-2= a human colon carcinoma cell line, MDCK= Madin-Darby canine kidney cell line, PSA= Polar surface area.

References and notes

1. D. K. Yadav and F. Khan, *J. Chemometrics*, 2013, **27**, 21–33.
2. D. K. Yadav, K. Kalani, A. K. Singh, F. Khan, S. K. Srivastava and A. B. Pant, *Curr. Med. Chem.*, 2013, **21**, 1160-1170.
3. D. K. Yadav, K. Kalani, F. Khan and S. K. Srivastava, *Med. Chem.* 2013, **9**, 1073–1084.
4. SMART & SAINT. Software Reference manuals. Versions 6.28a & 5.625, Bruker Analytical X-ray Systems Inc., Madison, Wisconsin, U.S.A., (2001).
5. G. M. Sheldrick, SHELXS97 and SHELXL97, Programs for crystal structure solution and refinement; University of Gottingen: Germany, (1997).

^{1}H NMR SPECTRA of 3 (300 MHz, $CDCl_3$):

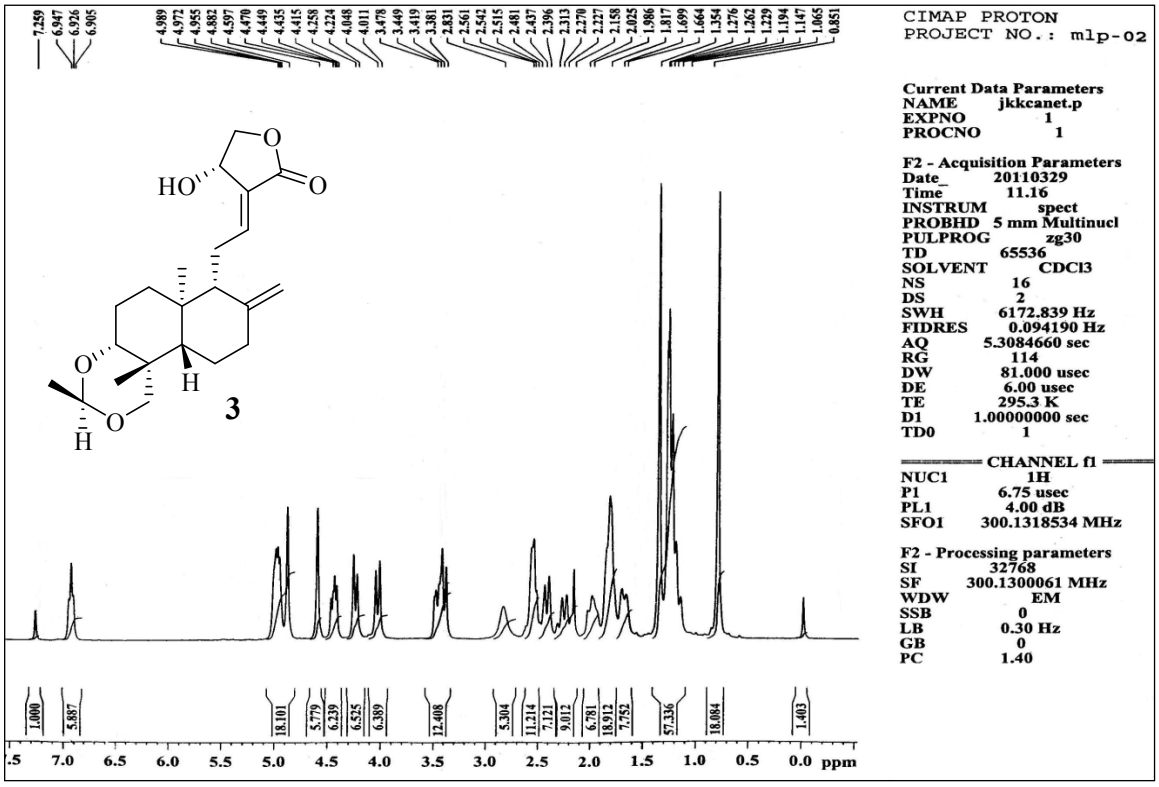

^{13}C NMR SPECTRA of 3 (75 MHz, $CDCl_3$):

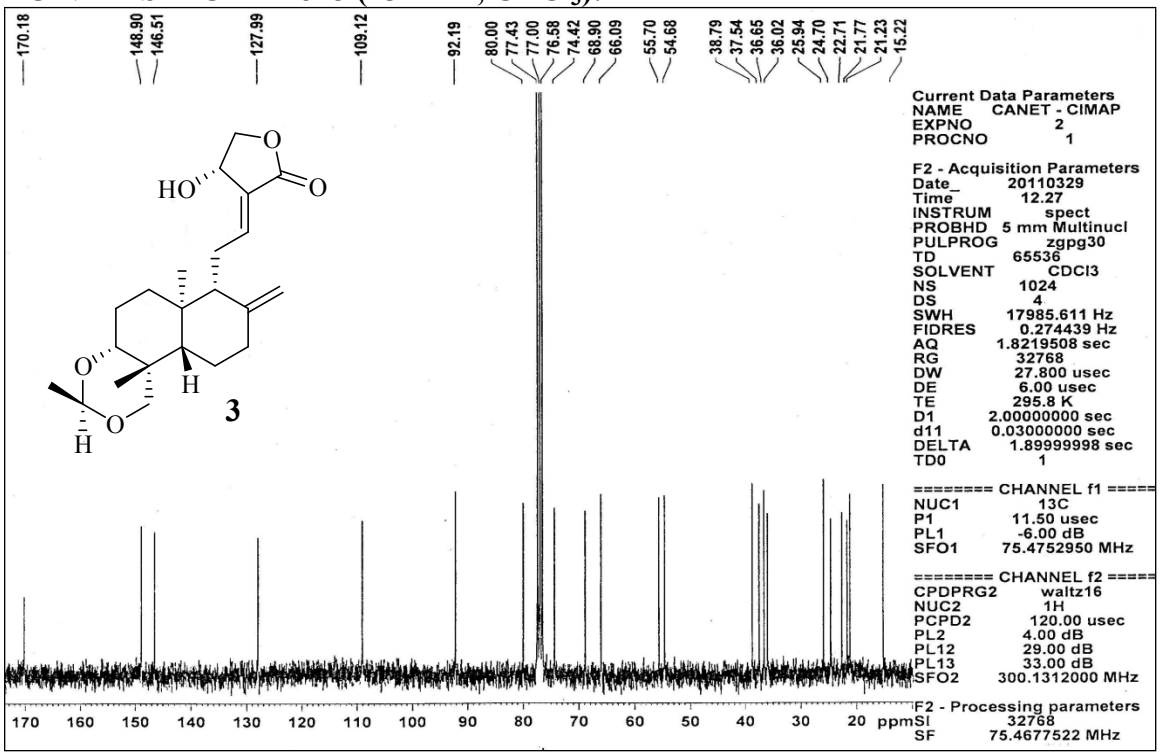

DEPT 135 of 3 (75 MHz, $CDCl_3$):

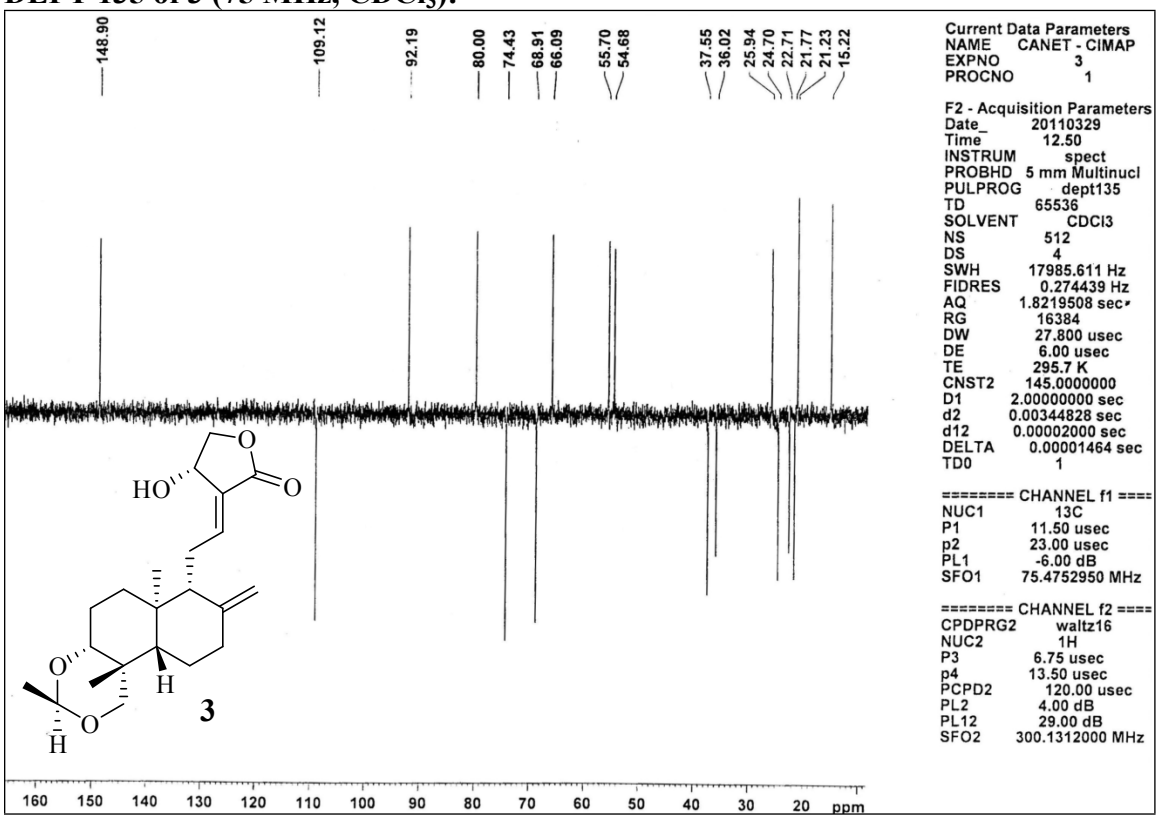

ESI-MASS SPECTRA of 3:

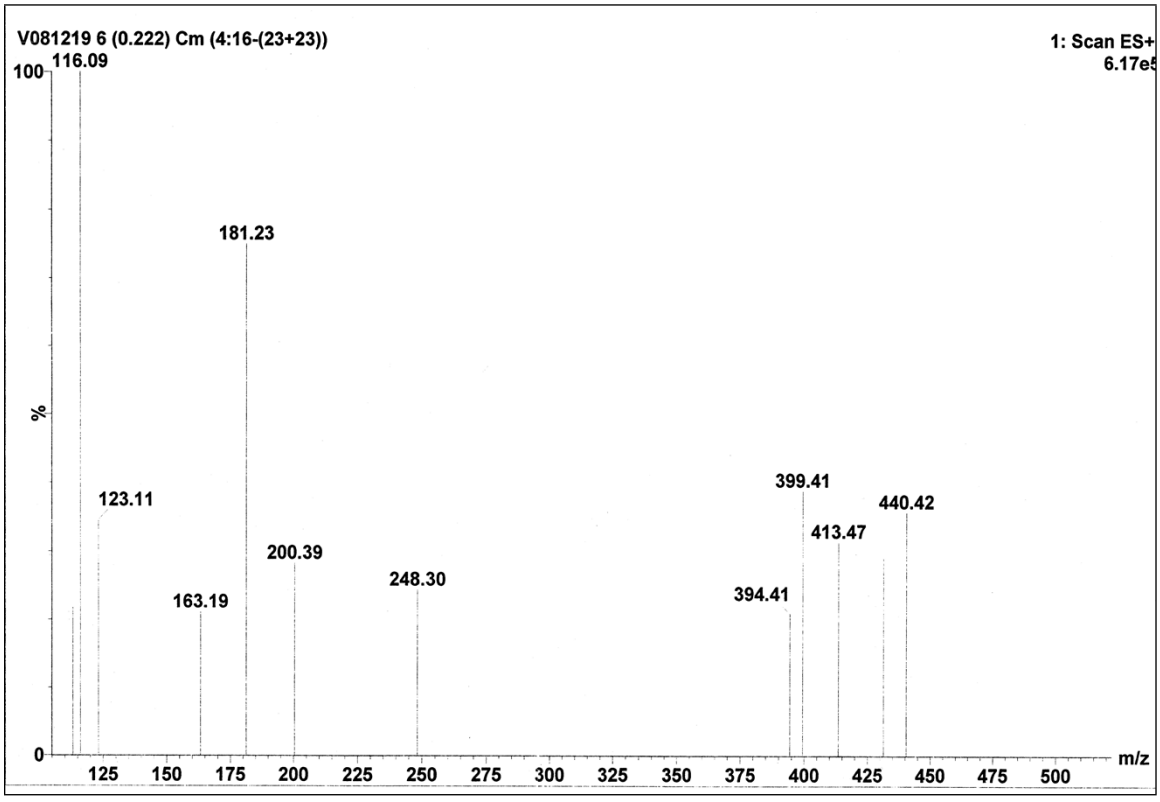

IR SPECTRA of 3 (KBr):

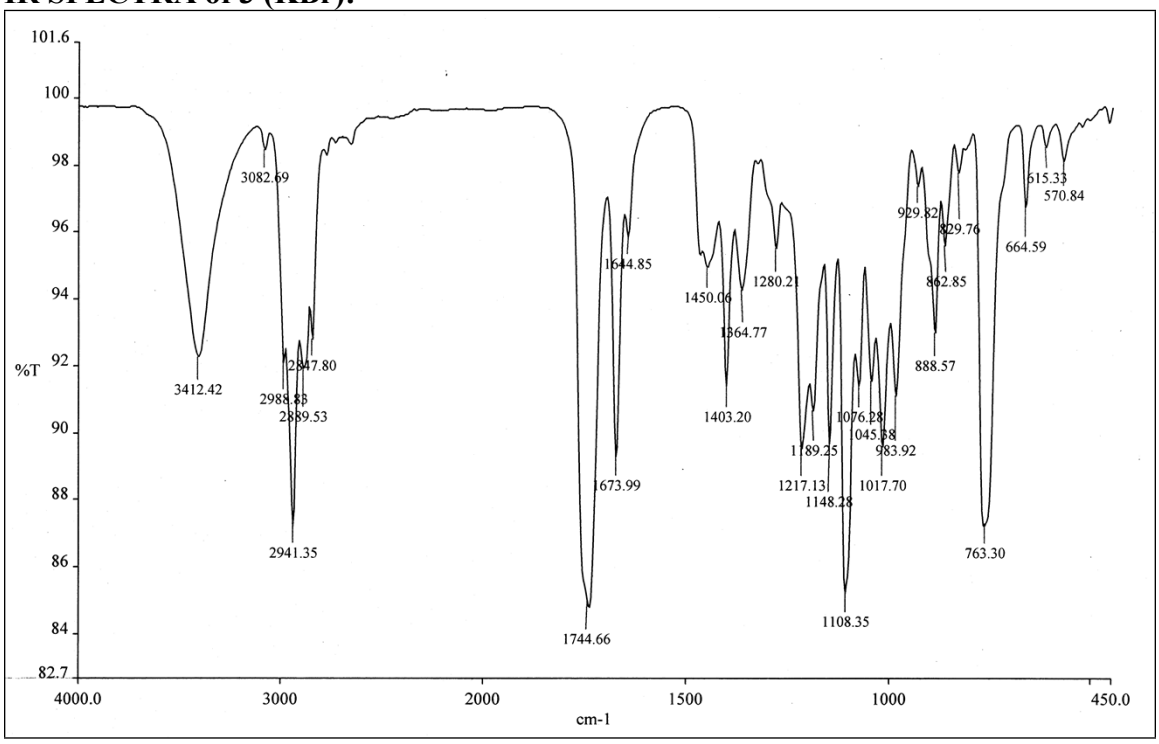

^{1}H NMR SPECTRA of 4 (300 MHz, $CDCl_3$):

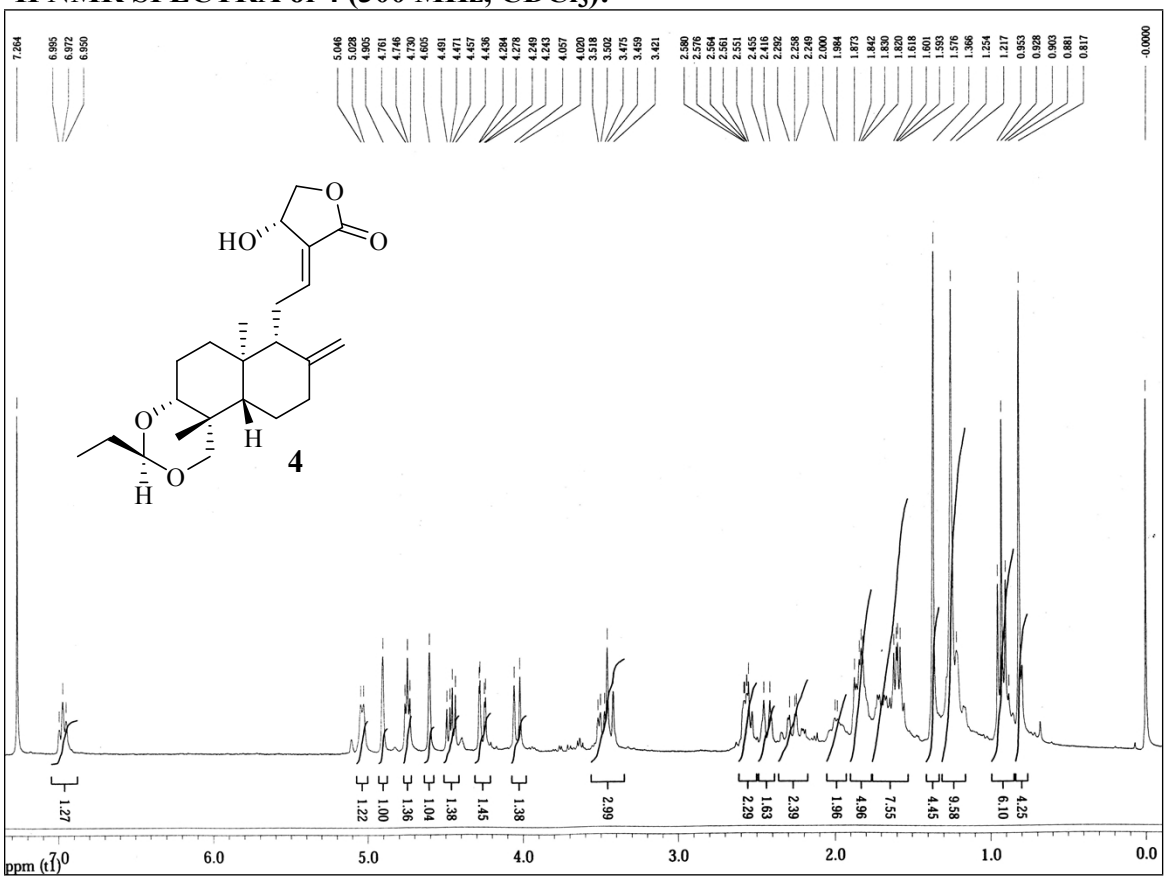

ESI-MASS SPECTRA of 4:

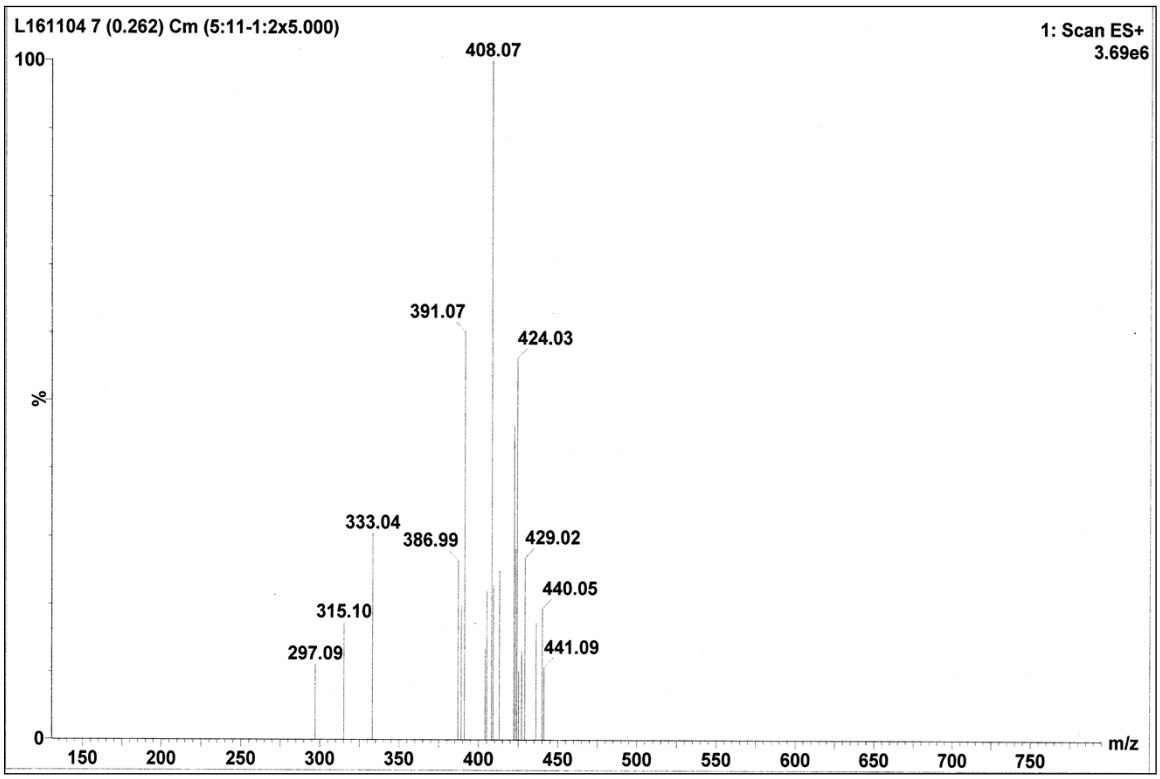

IR SPECTRA of 4 (KBr):

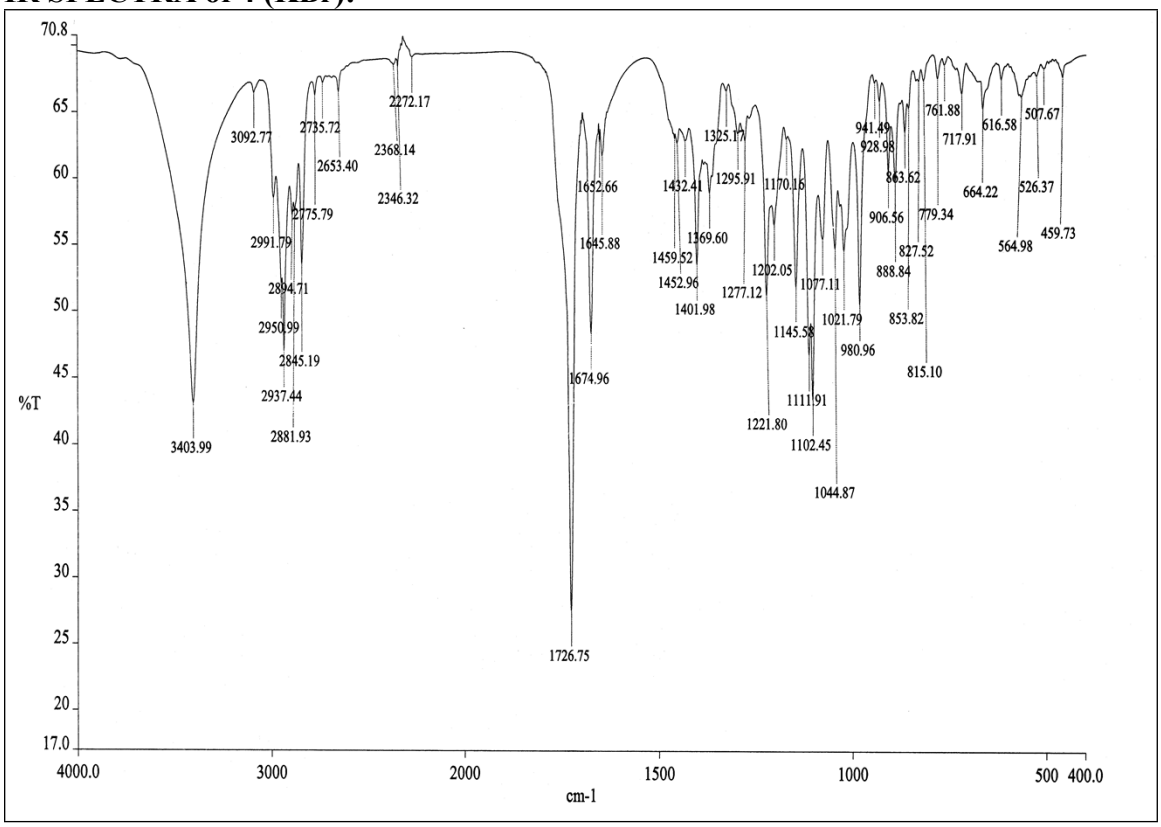

^{1}H NMR SPECTRA of 5 (300 MHz, $CDCl_3$):

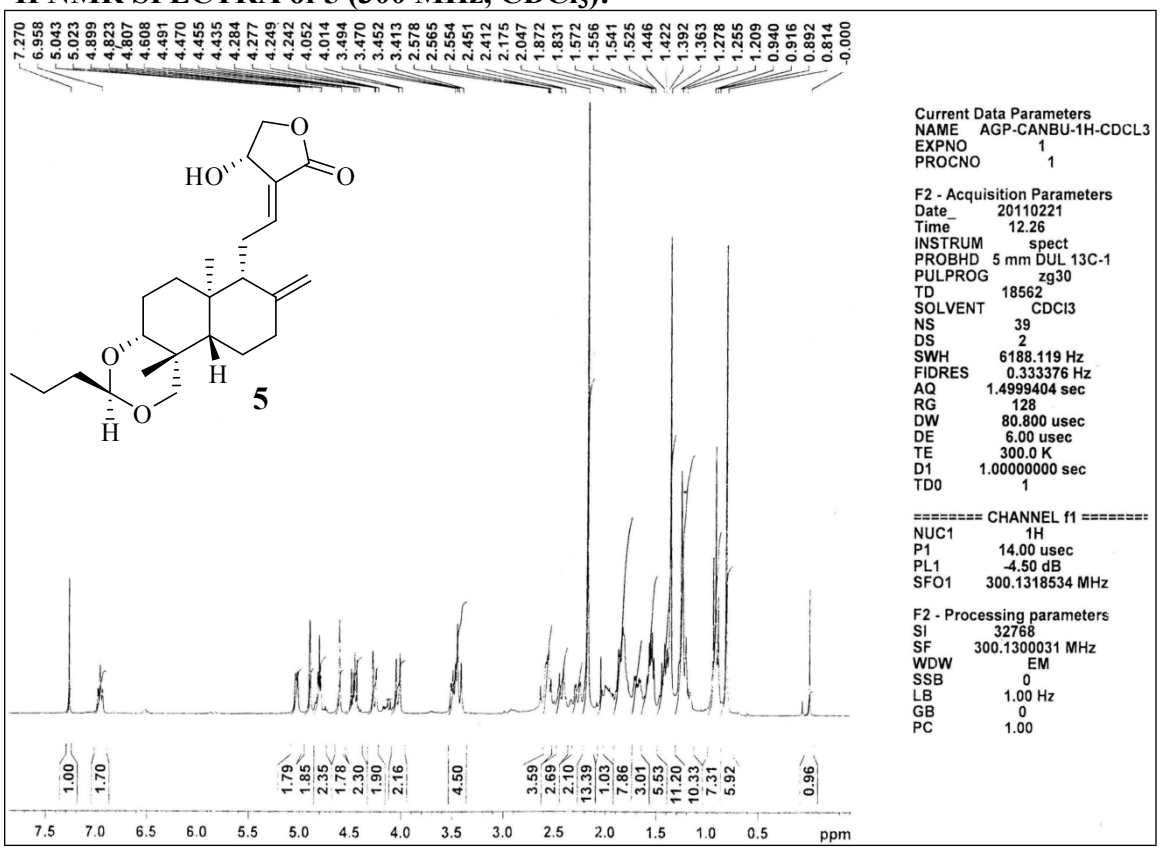

ESI-MASS SPECTRA of 5:

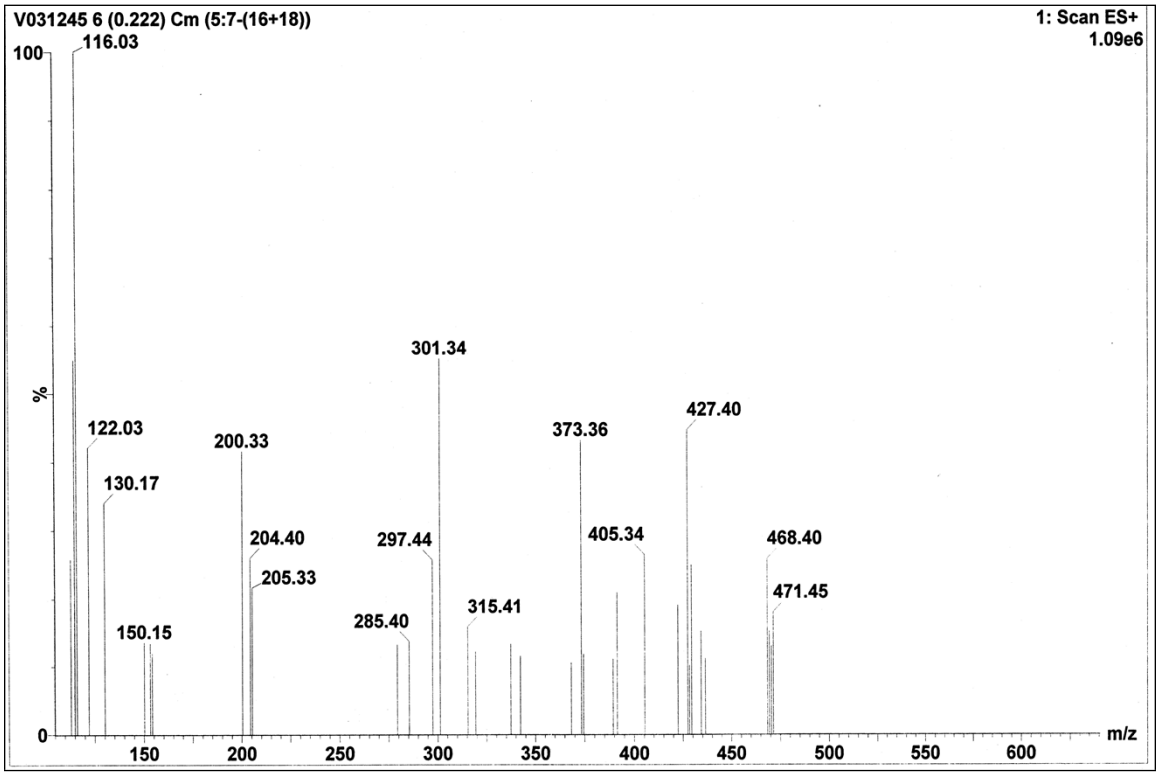

^{1}H NMR SPECTRA of 6 (300 MHz, $CDCl_3$):

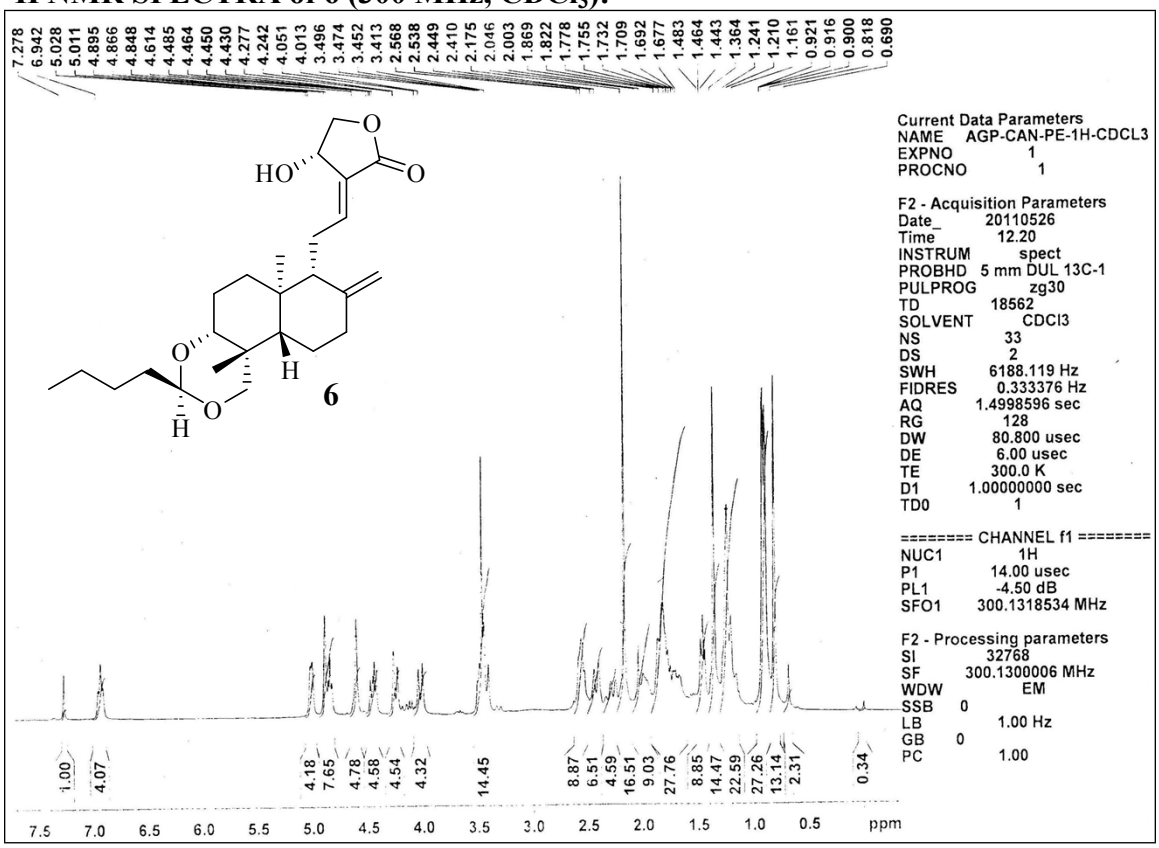

ESI-MASS SPECTRA of 6:

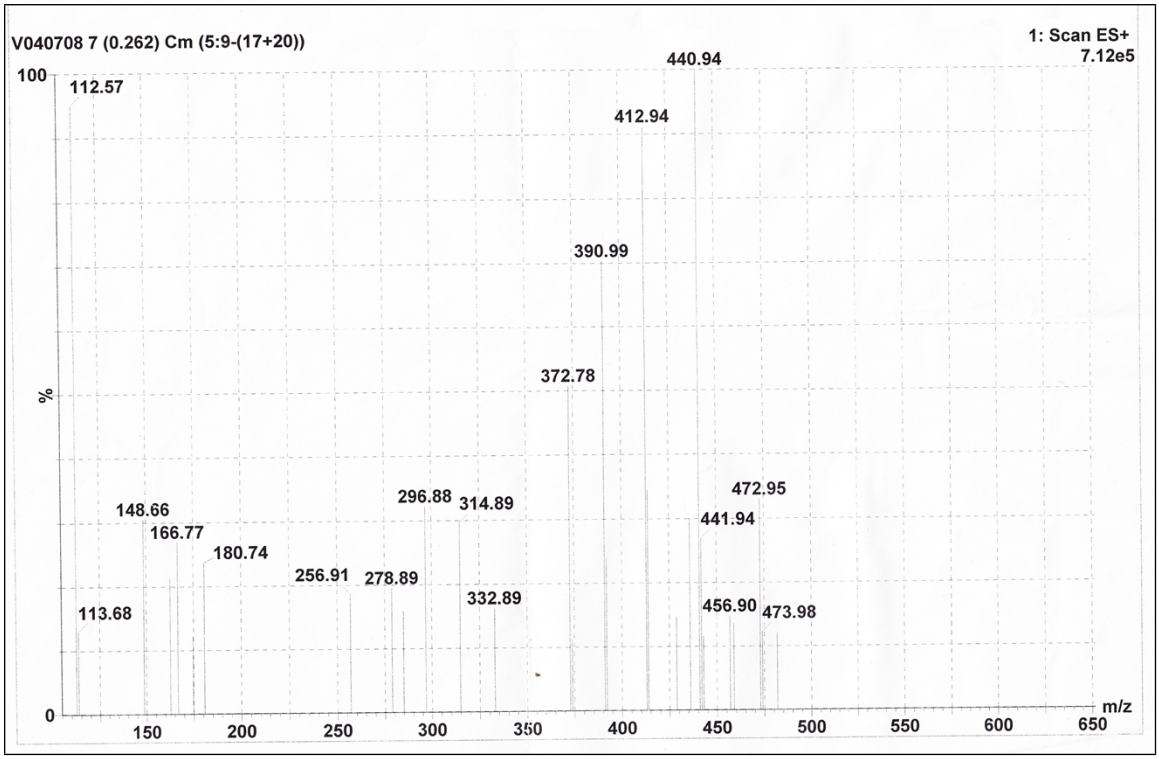

^{1}H NMR SPECTRA of 7 (300 MHz, $CDCl_3$):

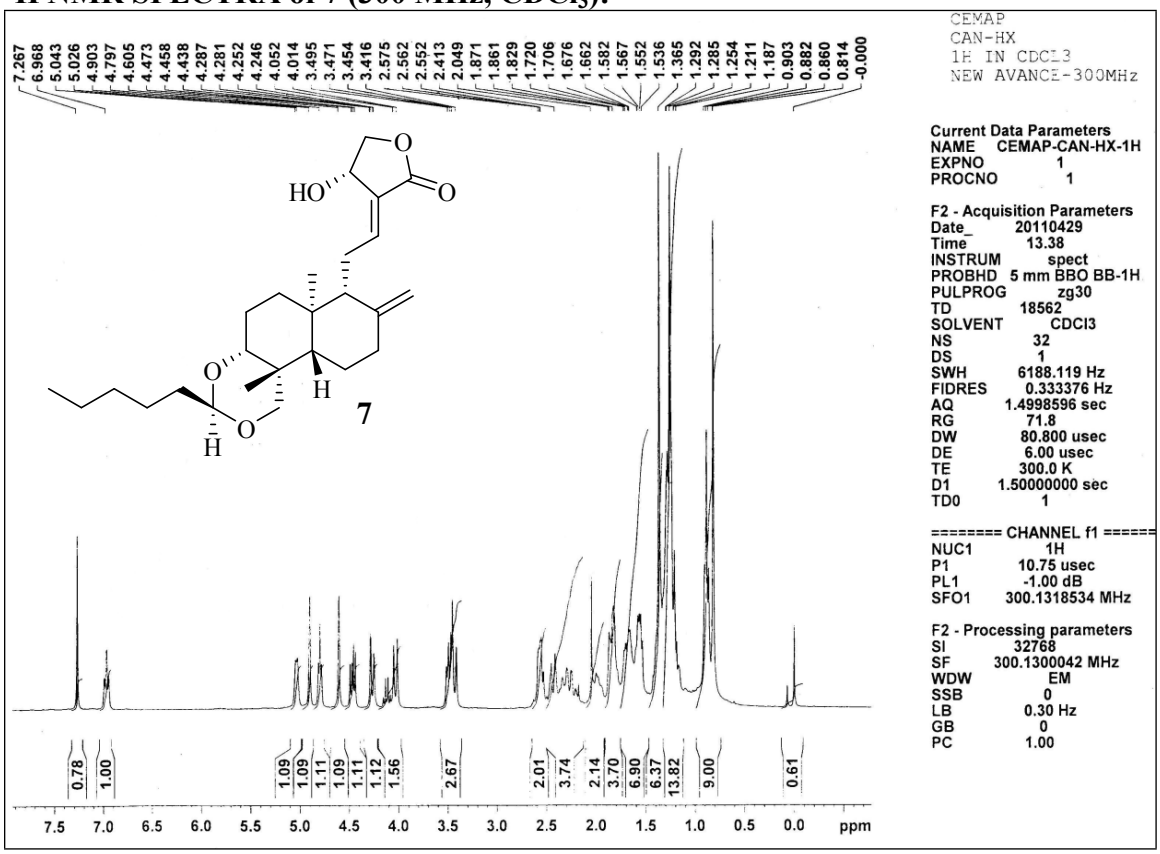

^{13}C NMR SPECTRA of 7 (75 MHz, $CDCl_3$):

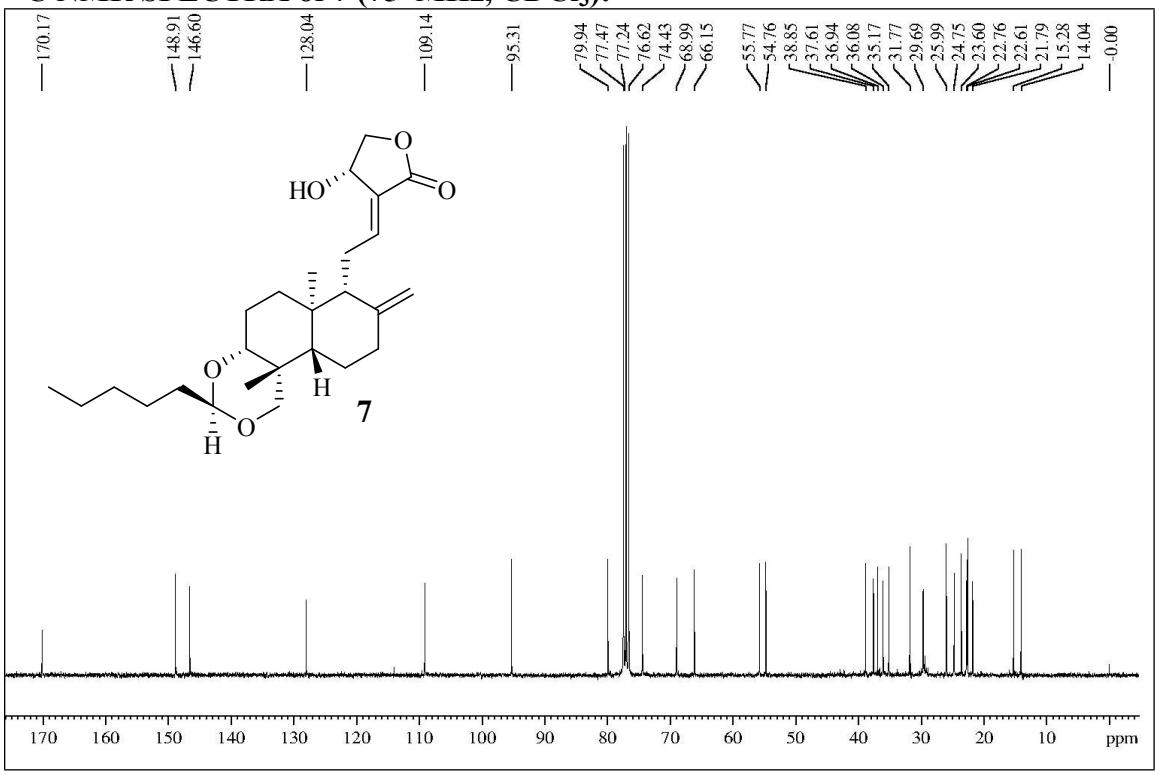

ESI-MASS SPECTRA of 7:

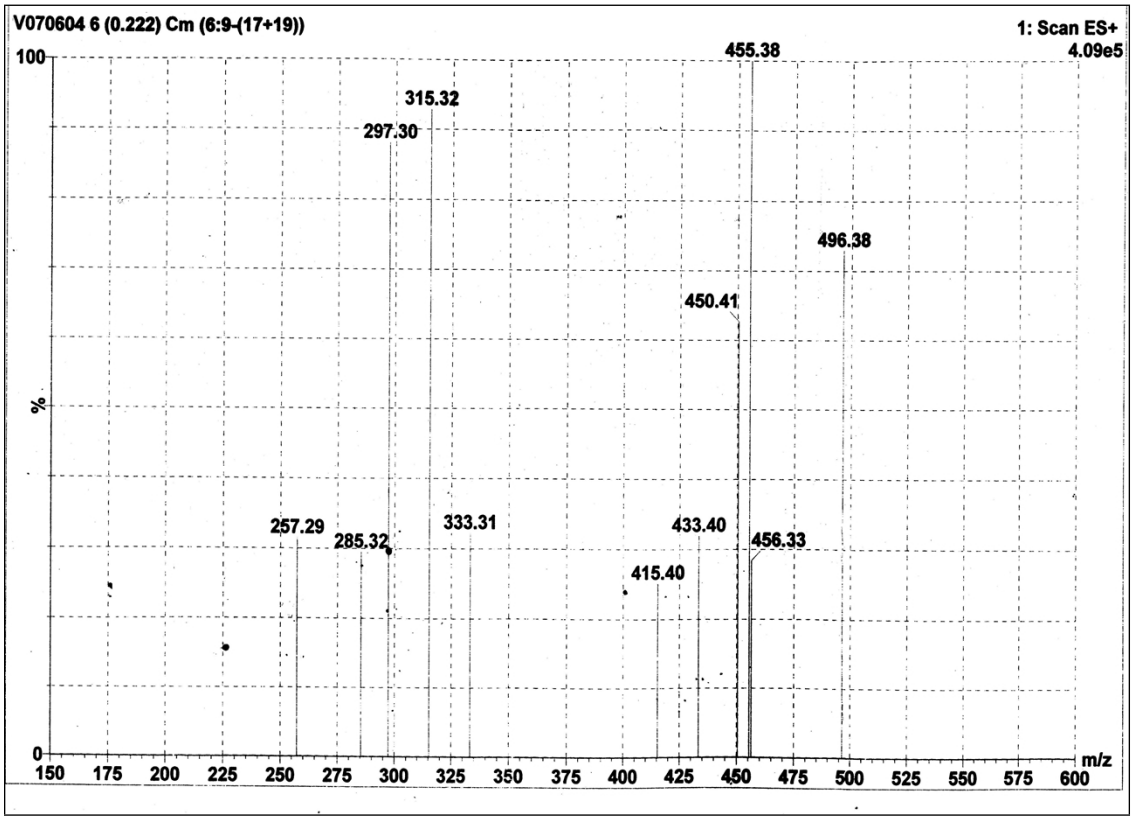

IR SPECTRA of 7 (KBr):

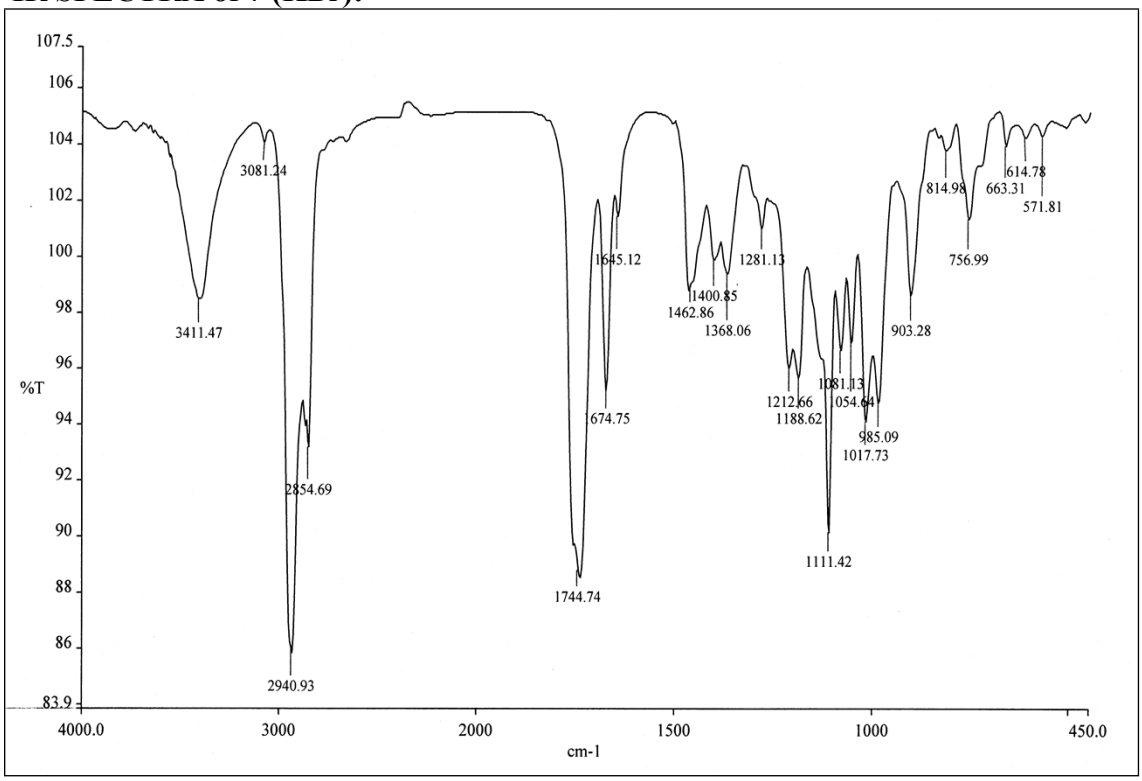

^{1}H NMR SPECTRA of 8 (300 MHz, $CDCl_3$):

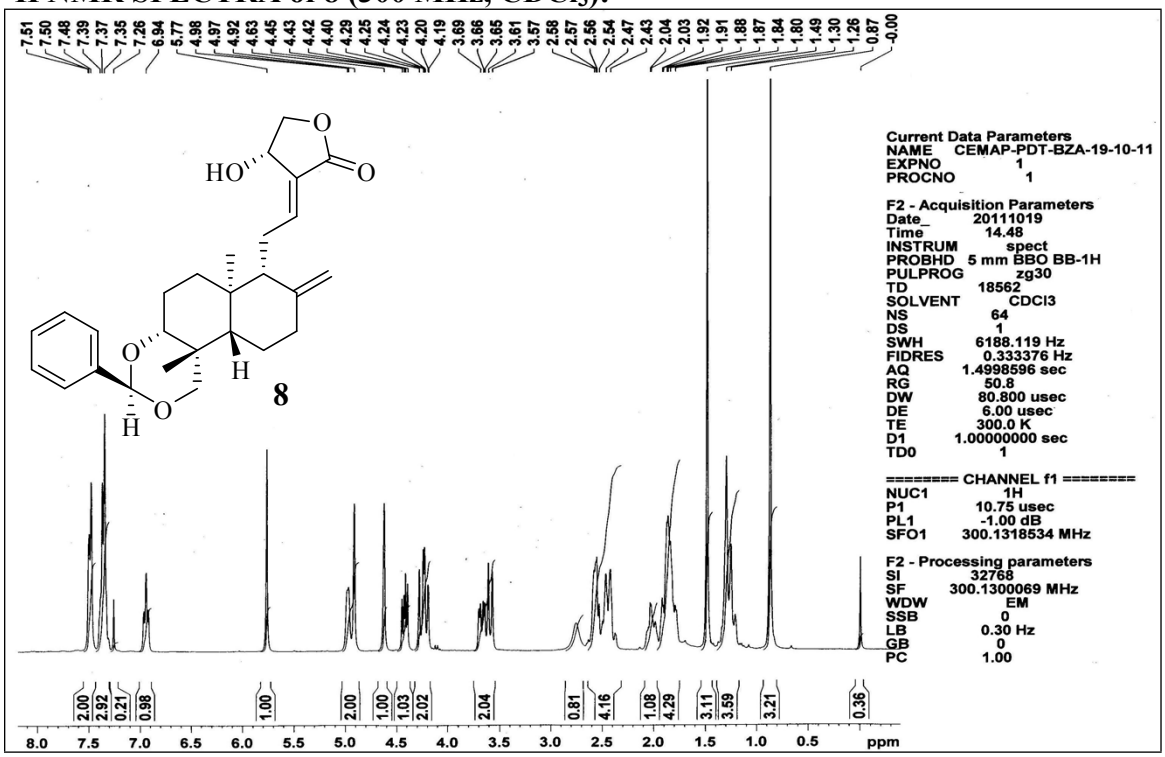

ESI-MASS SPECTRA of 8:

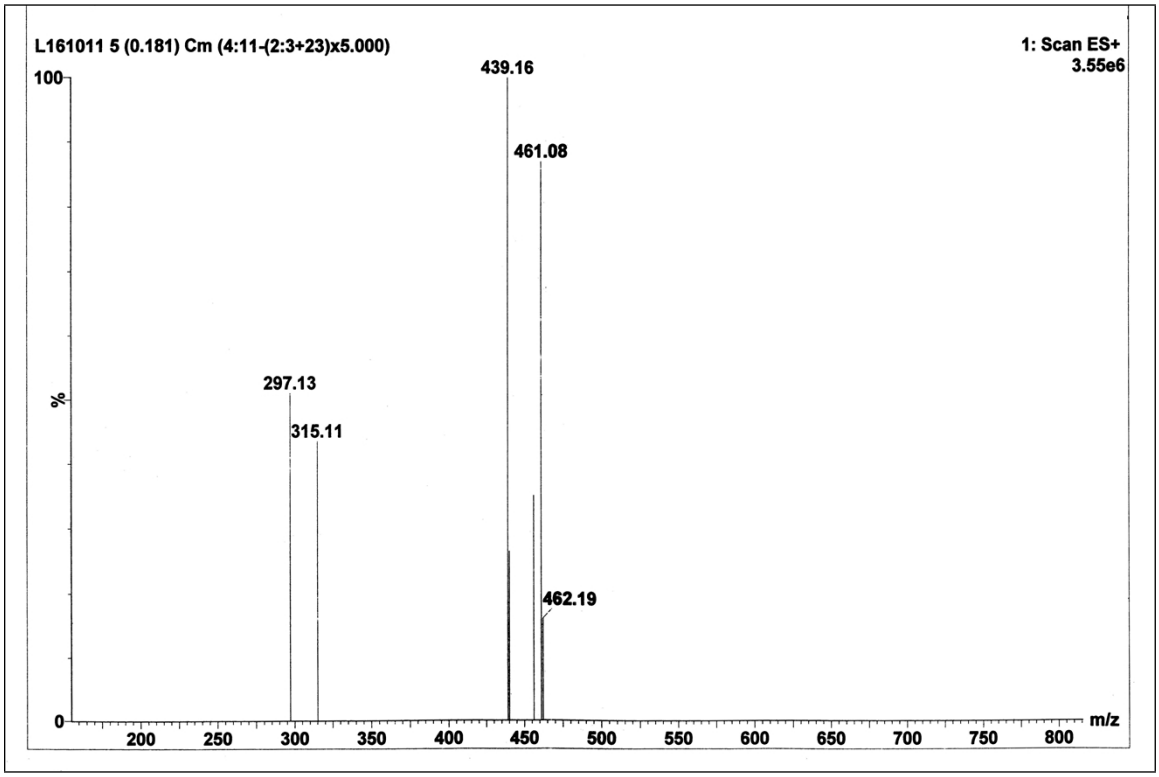

^{1}H NMR SPECTRA of 3a (300 MHz, $CDCl_3$):

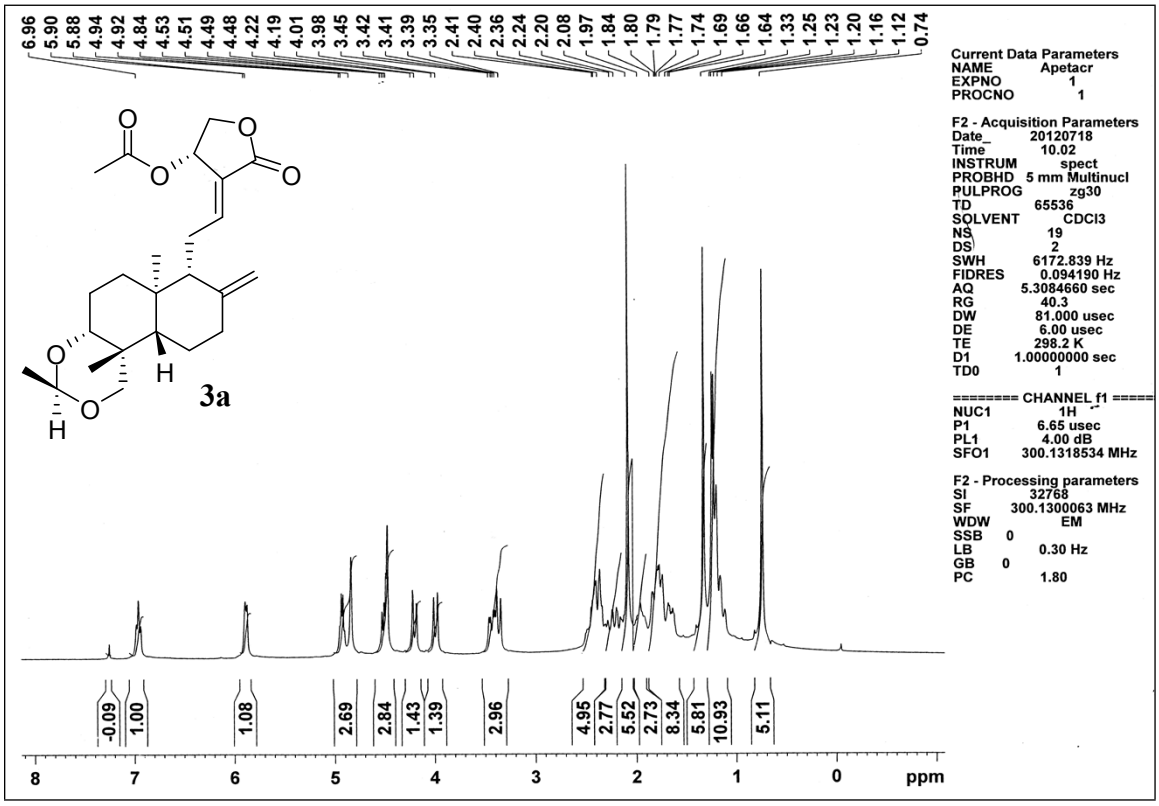

^{13}C NMR SPECTRA of 3a (75 MHz, $CDCl_3$):

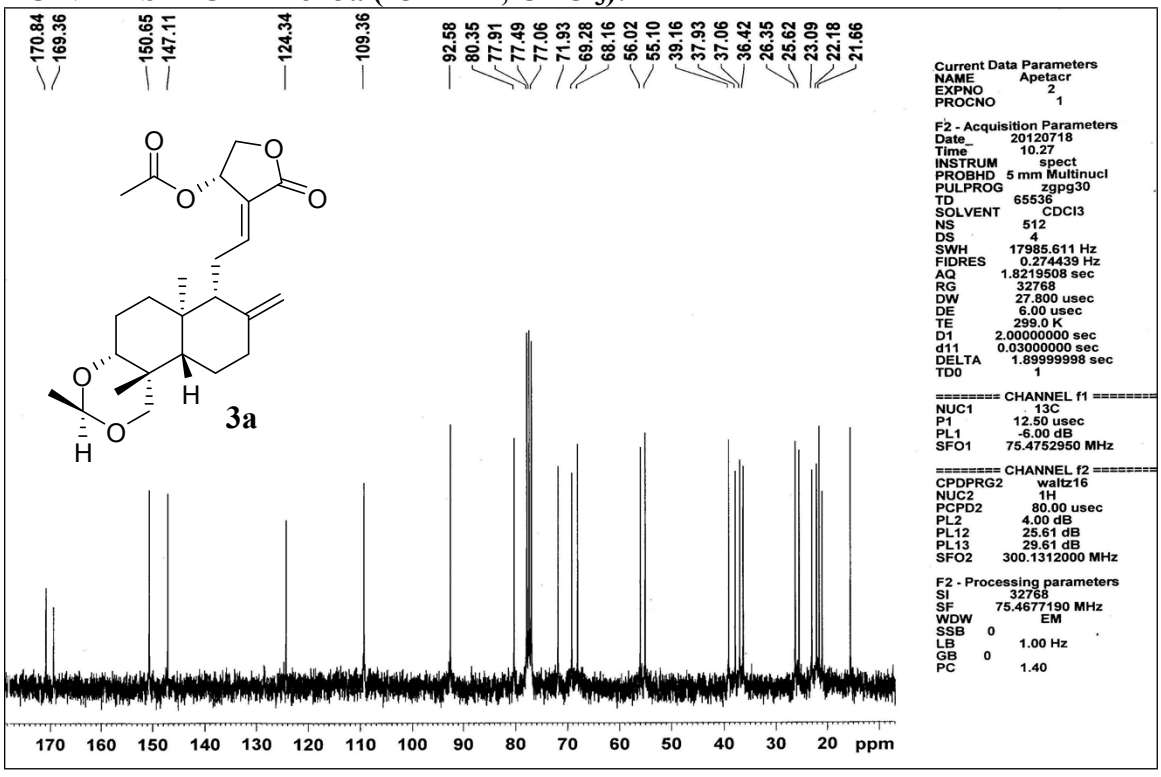

ESI mass SPECTRA of 3a:

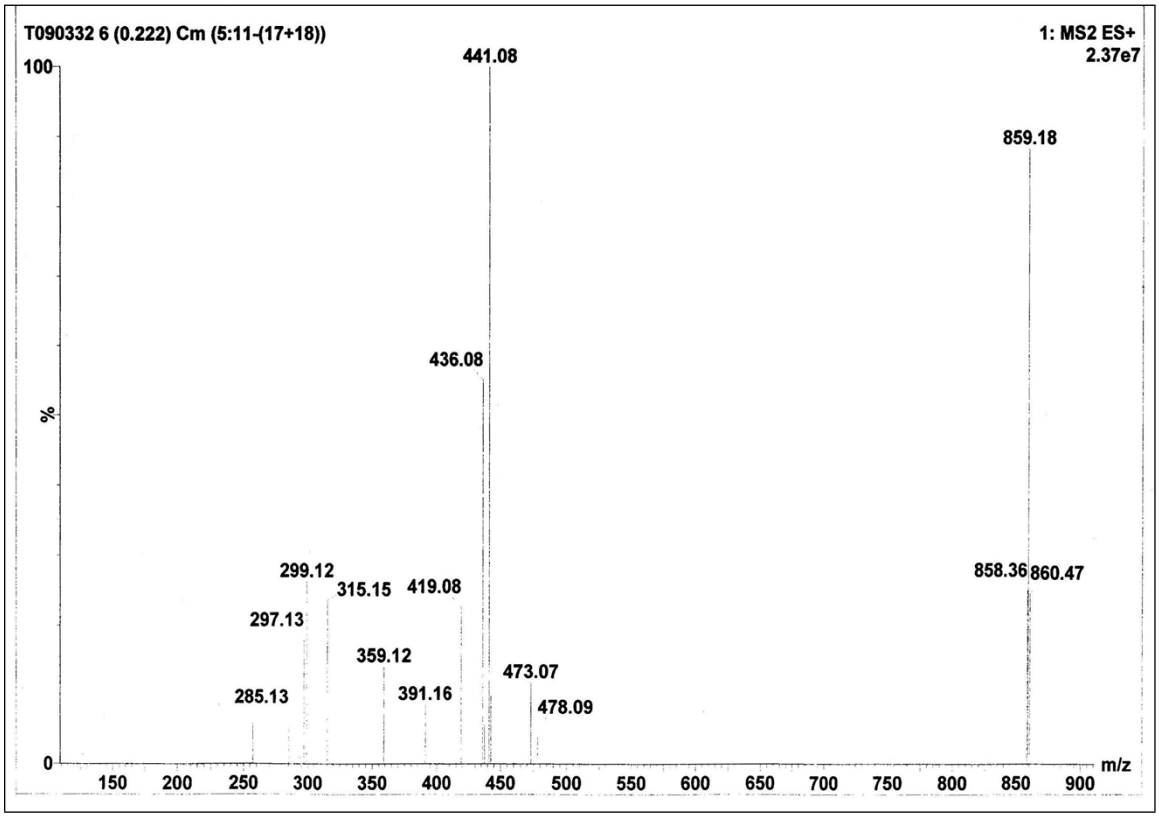

IR SPECTRA of 3a (KBr):

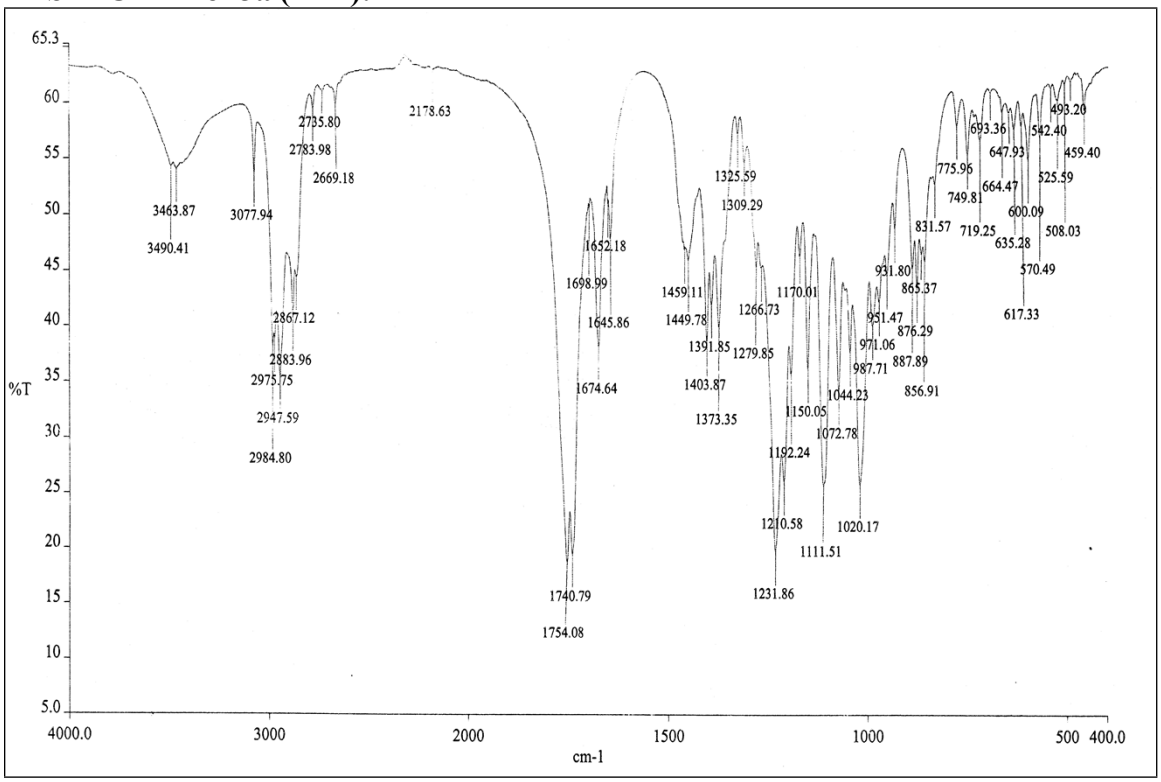

^{1}H NMR SPECTRA of 3b (300 MHz, $CDCl_3$):

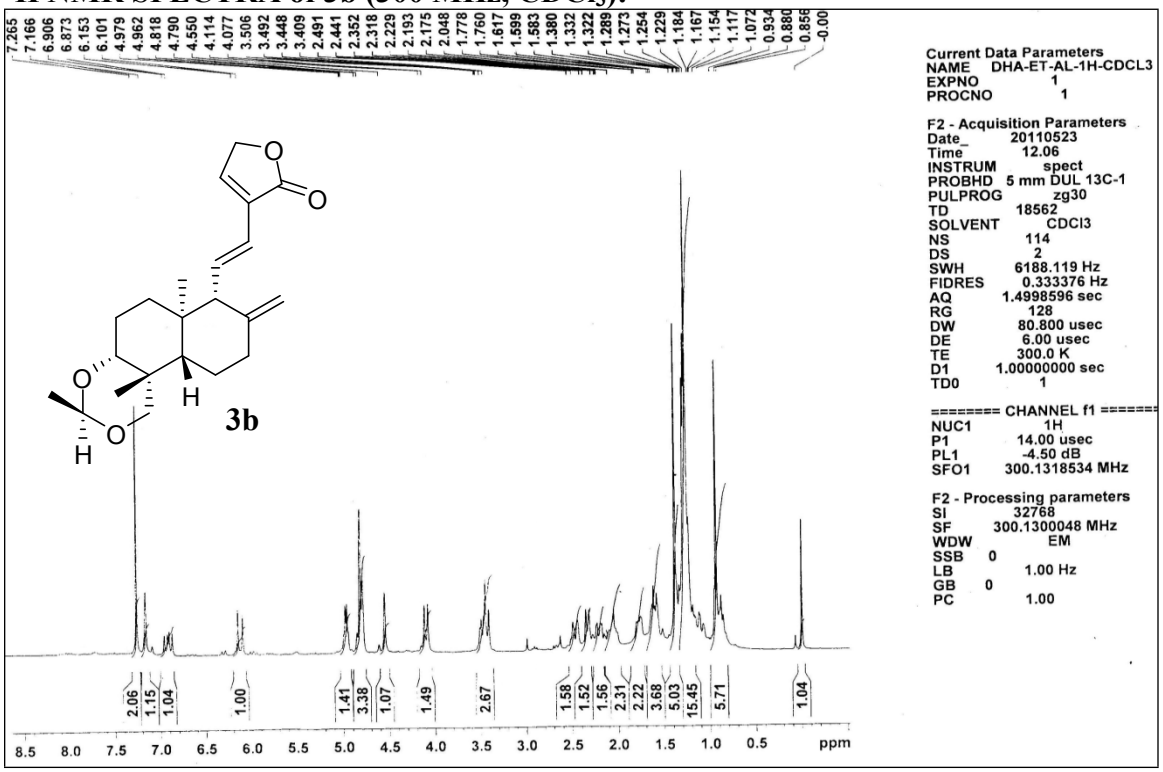

^{13}C NMR SPECTRA of 3b (75 MHz, $CDCl_3$):

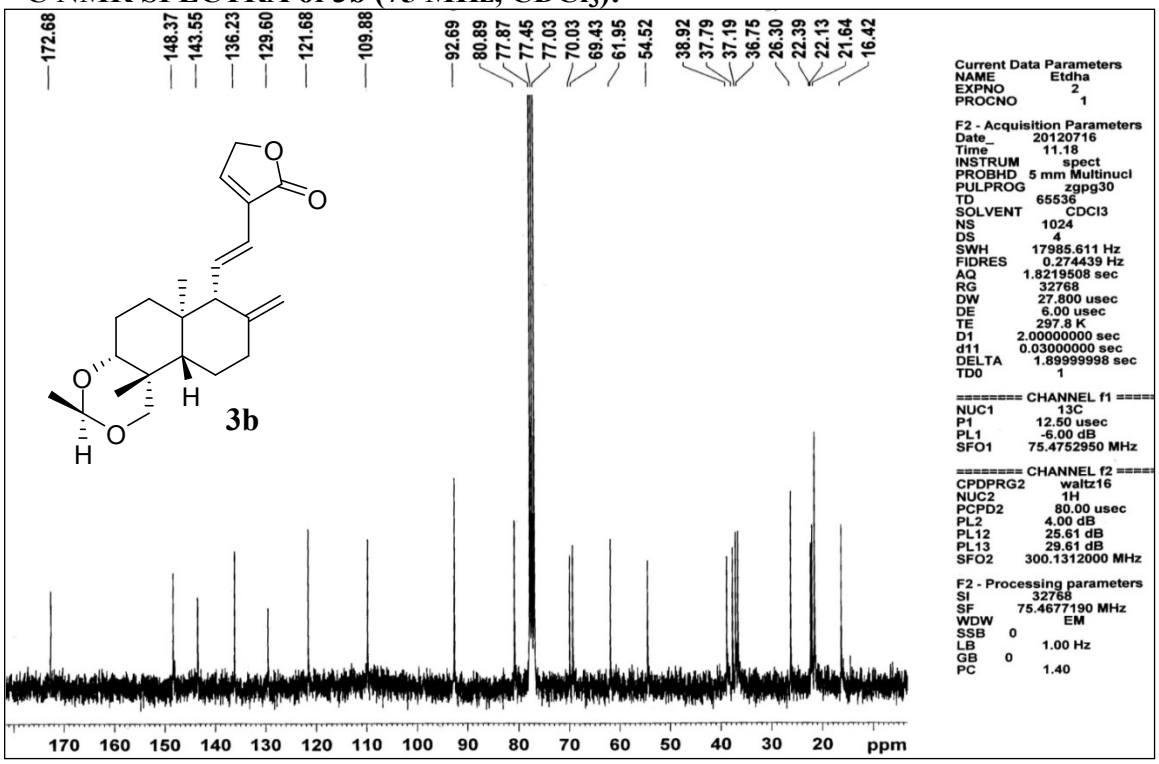

ESI-MASS SPECTRA of 3b:

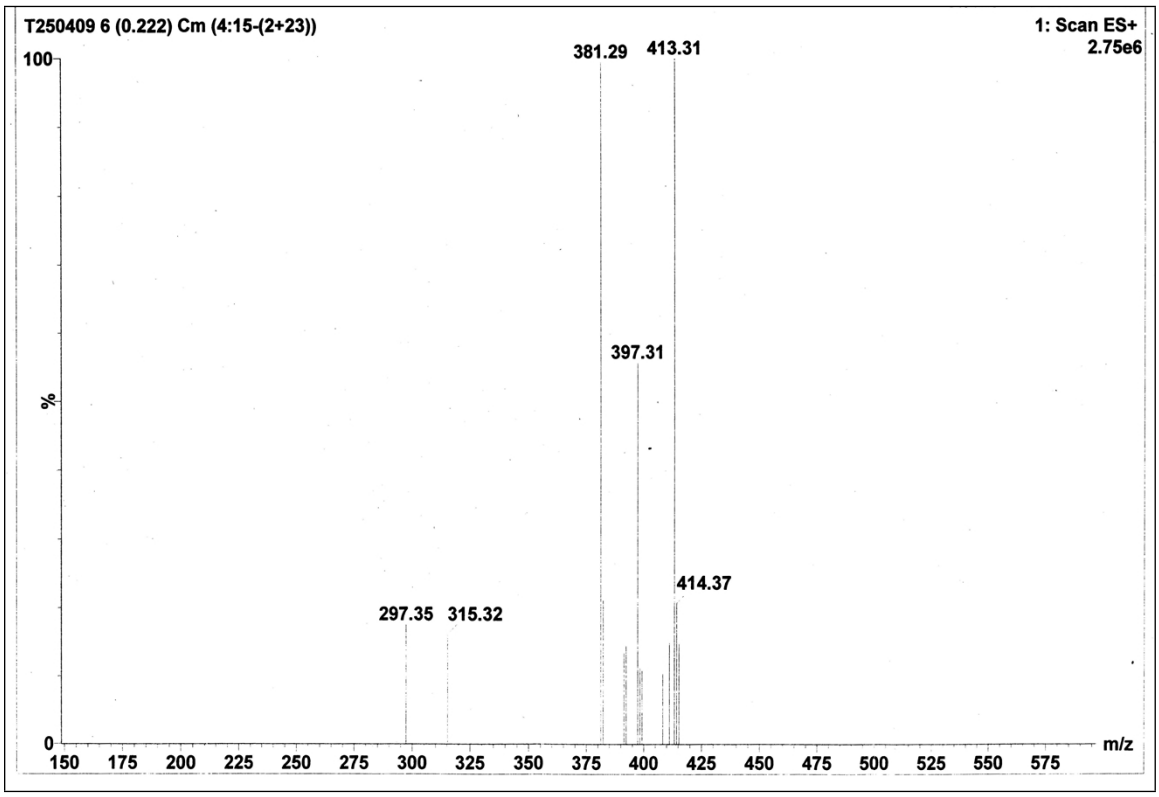

IR SPECTRA of 3b (KBr):

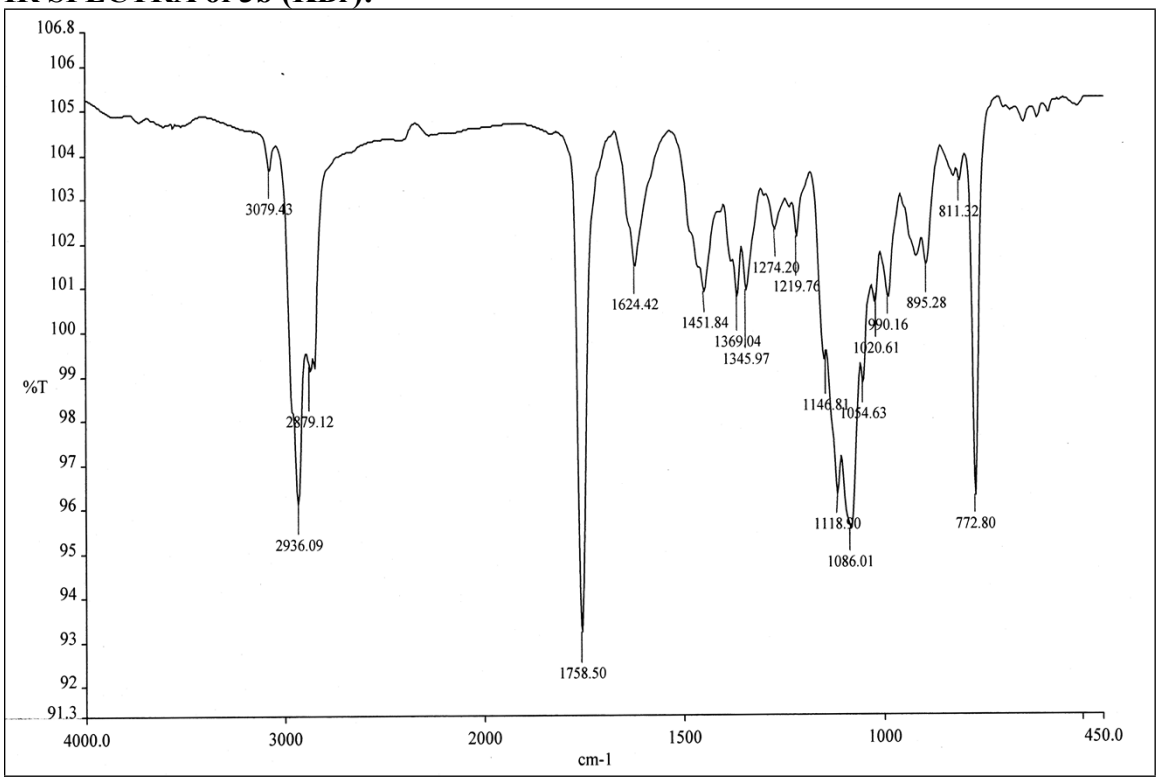

^{1}H NMR SPECTRA of 3c (300 MHz, $CDCl_3$):

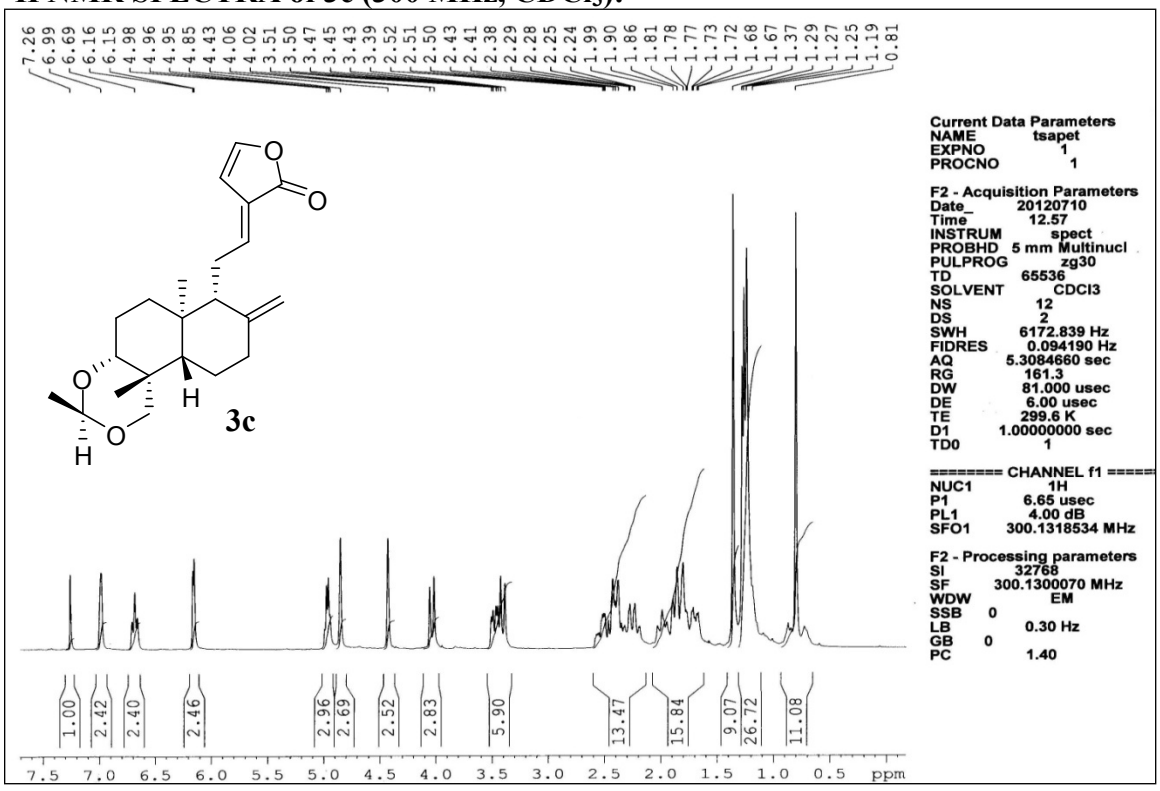

^{13}C NMR SPECTRA of 3c (75 MHz, $CDCl_3$):

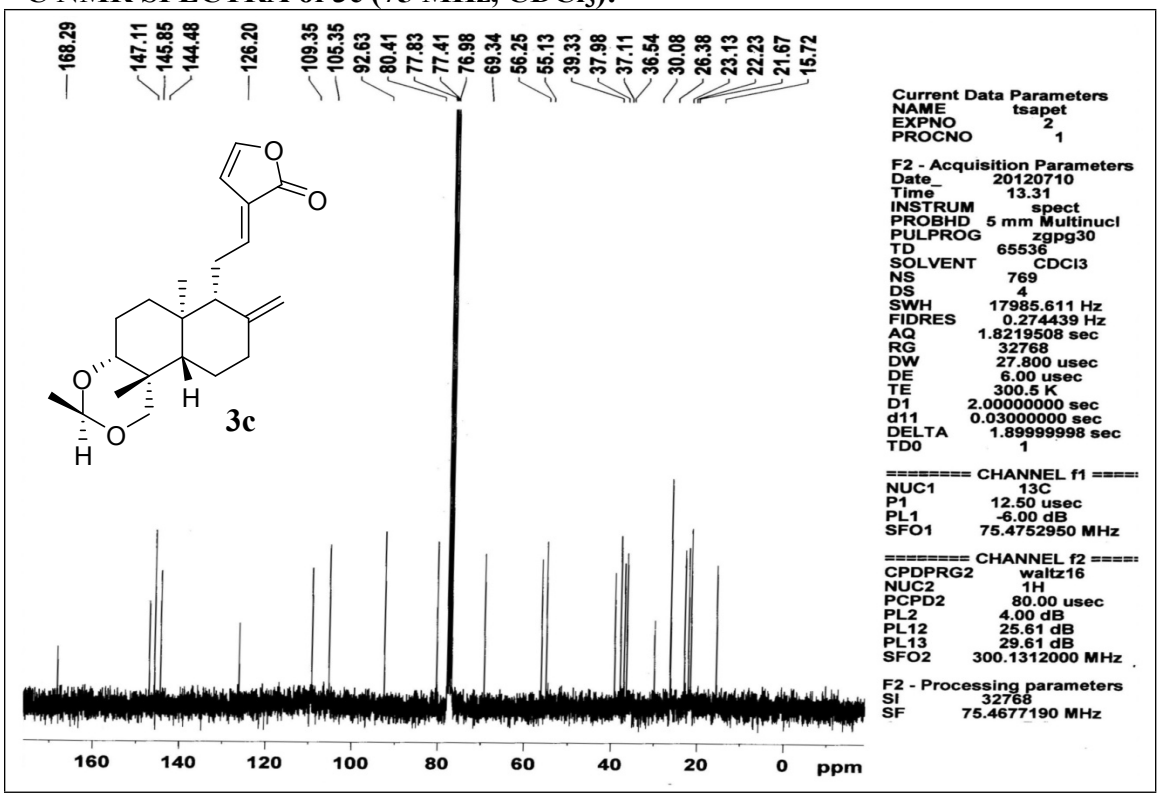

ESI-MASS SPECTRA of 3c:

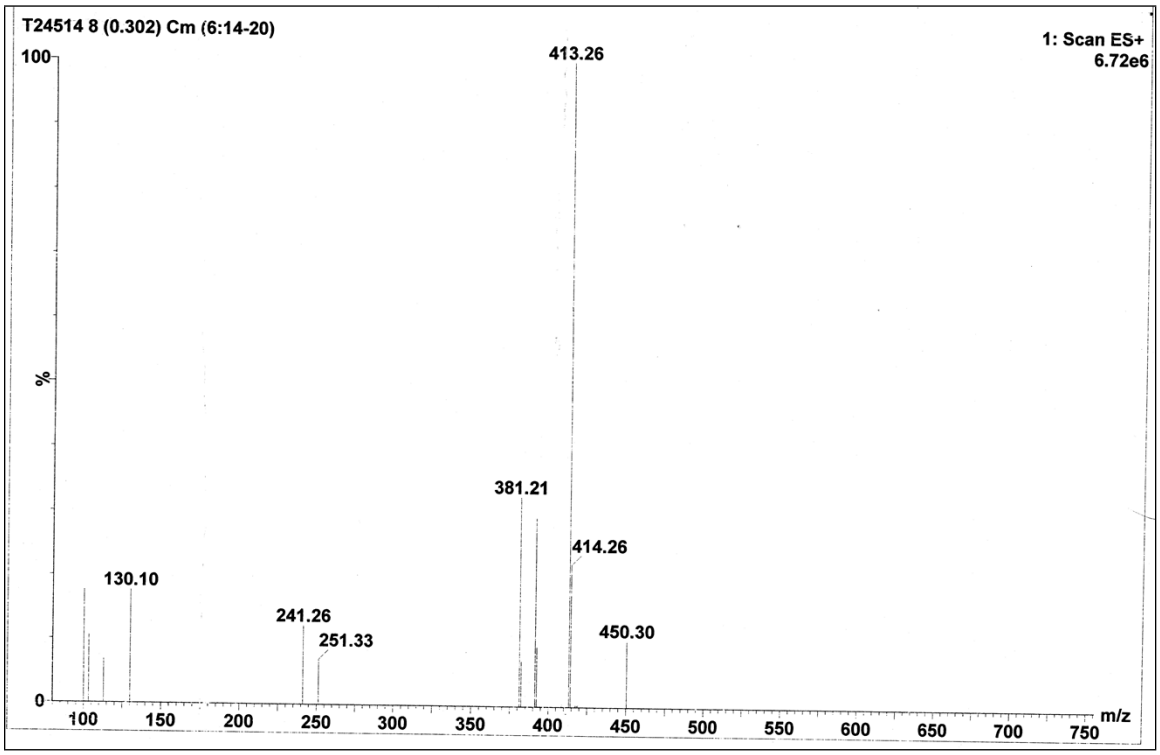

IR SPECTRA of 3c (KBr):

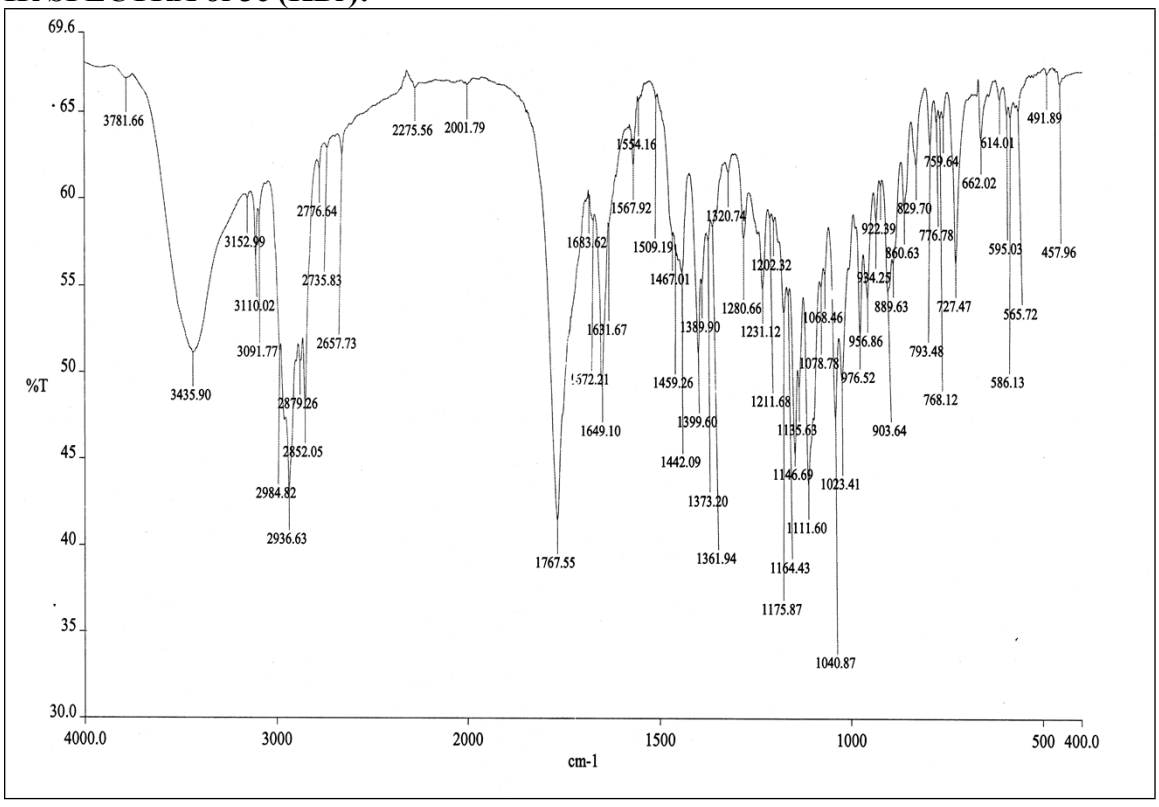

^{1}H NMR SPECTRA of 3d (300 MHz, $CDCl_3$):

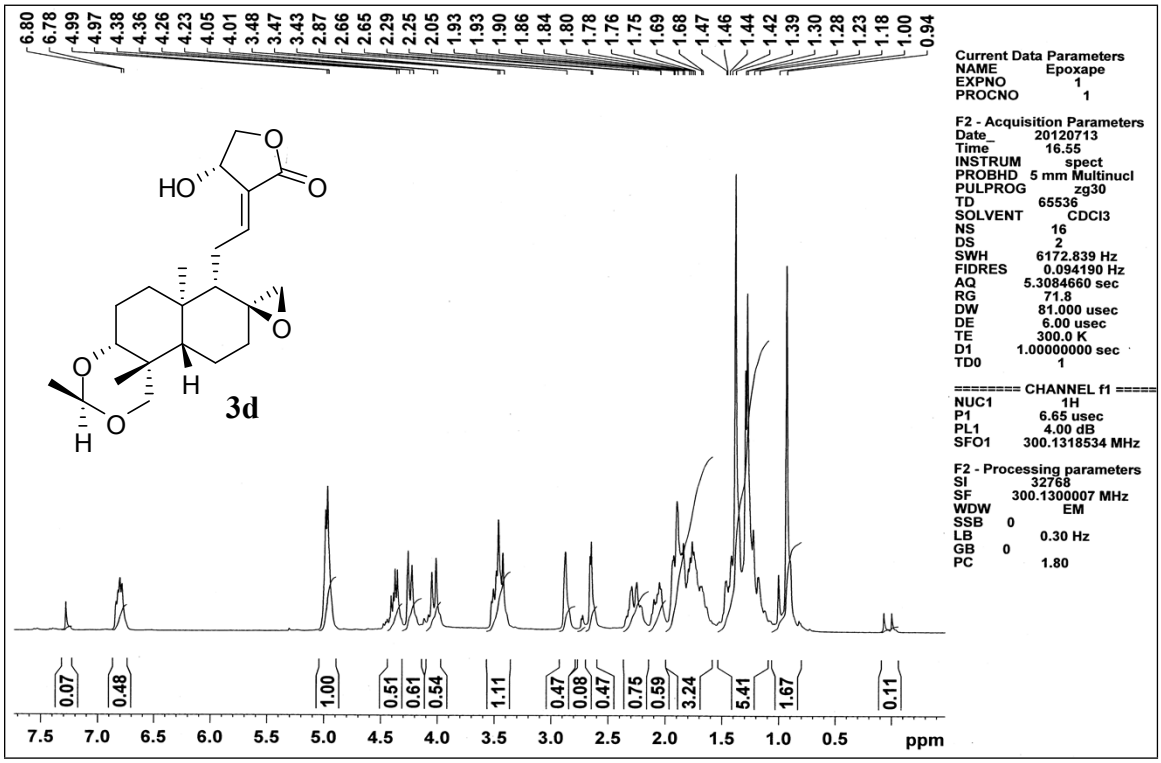

^{13}C NMR SPECTRA of 3d (75 MHz, $CDCl_3$):

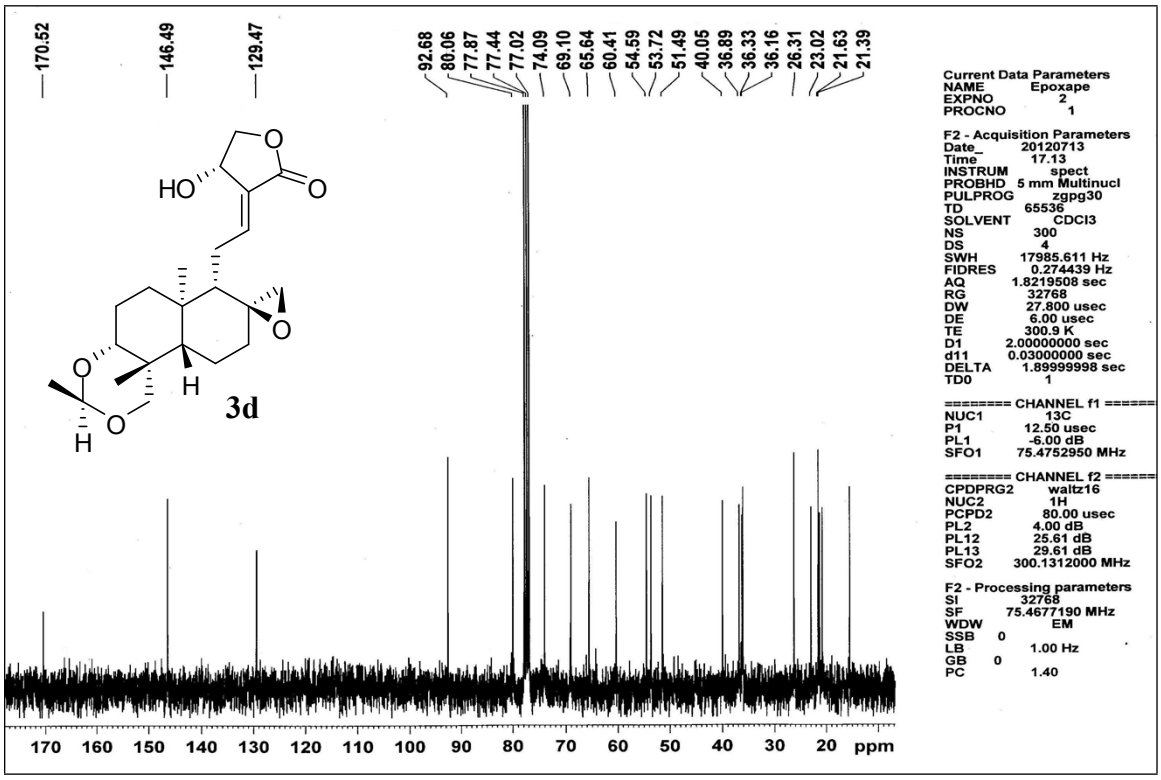

ESI-MASS SPECTRA of 3d:

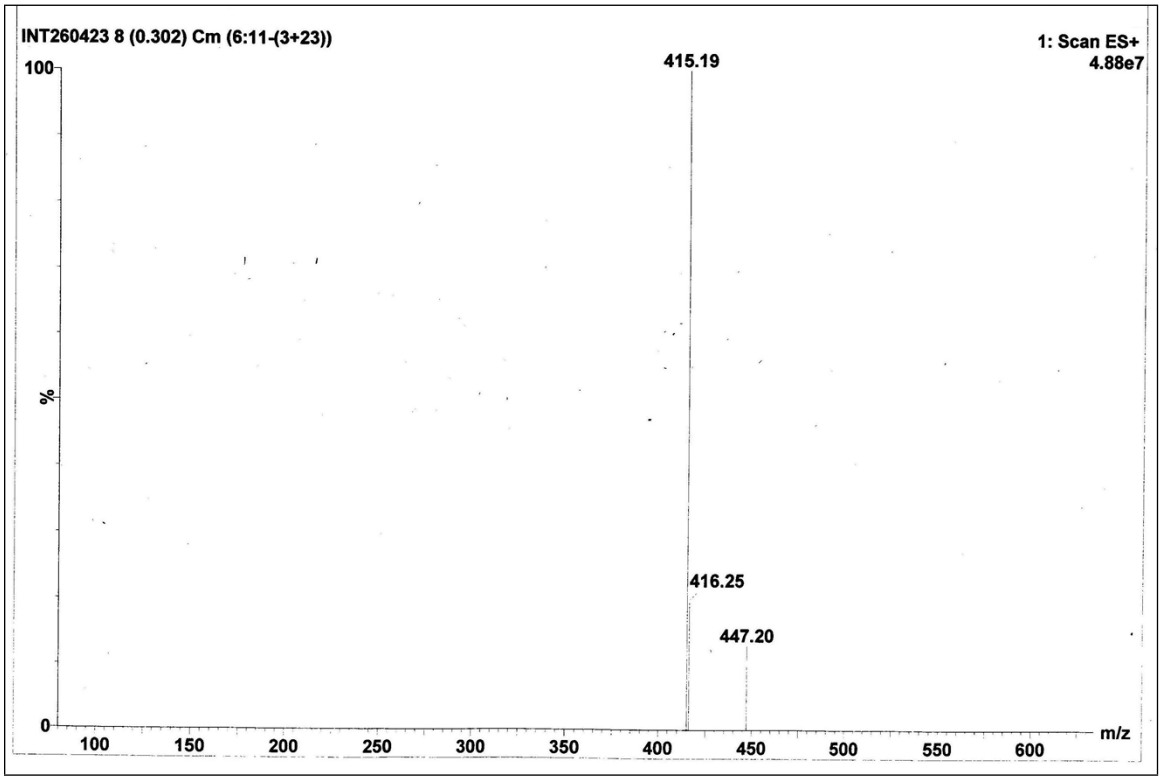

IR SPECTRA of 3d (KBr):

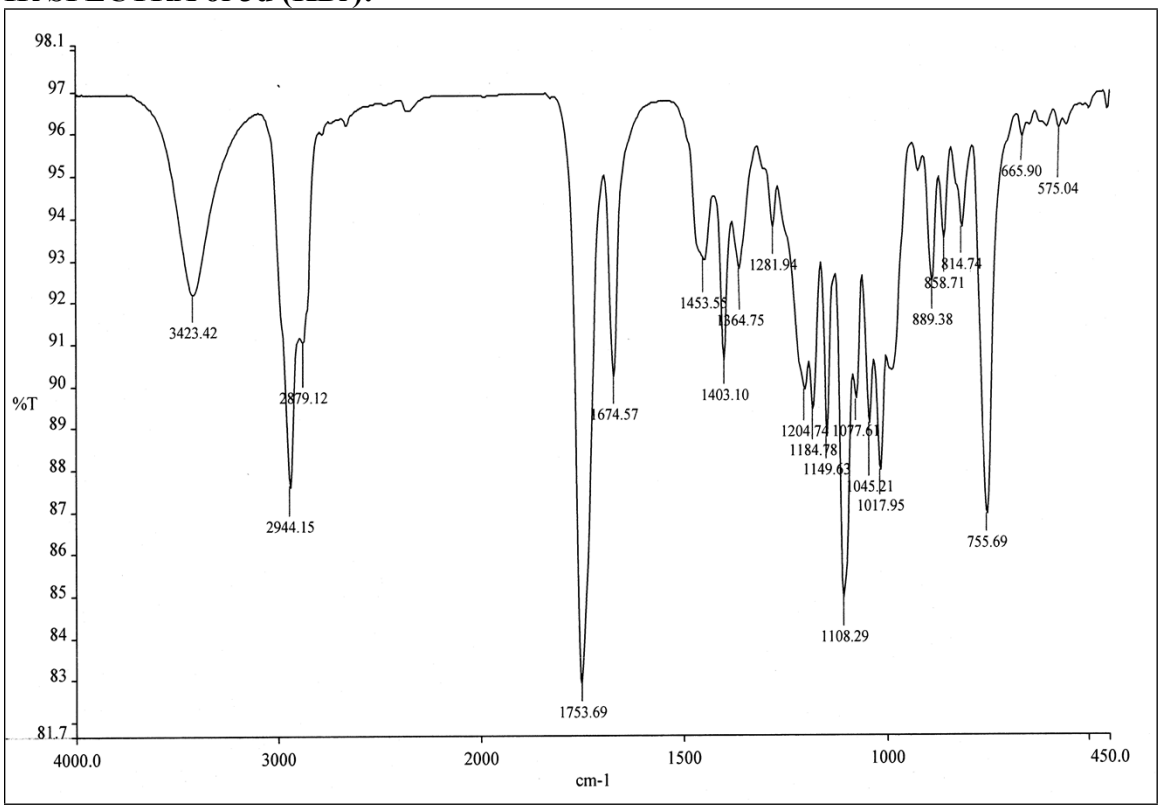

^{1}H NMR SPECTRA of 3e (400 MHz, DMSO-d6):

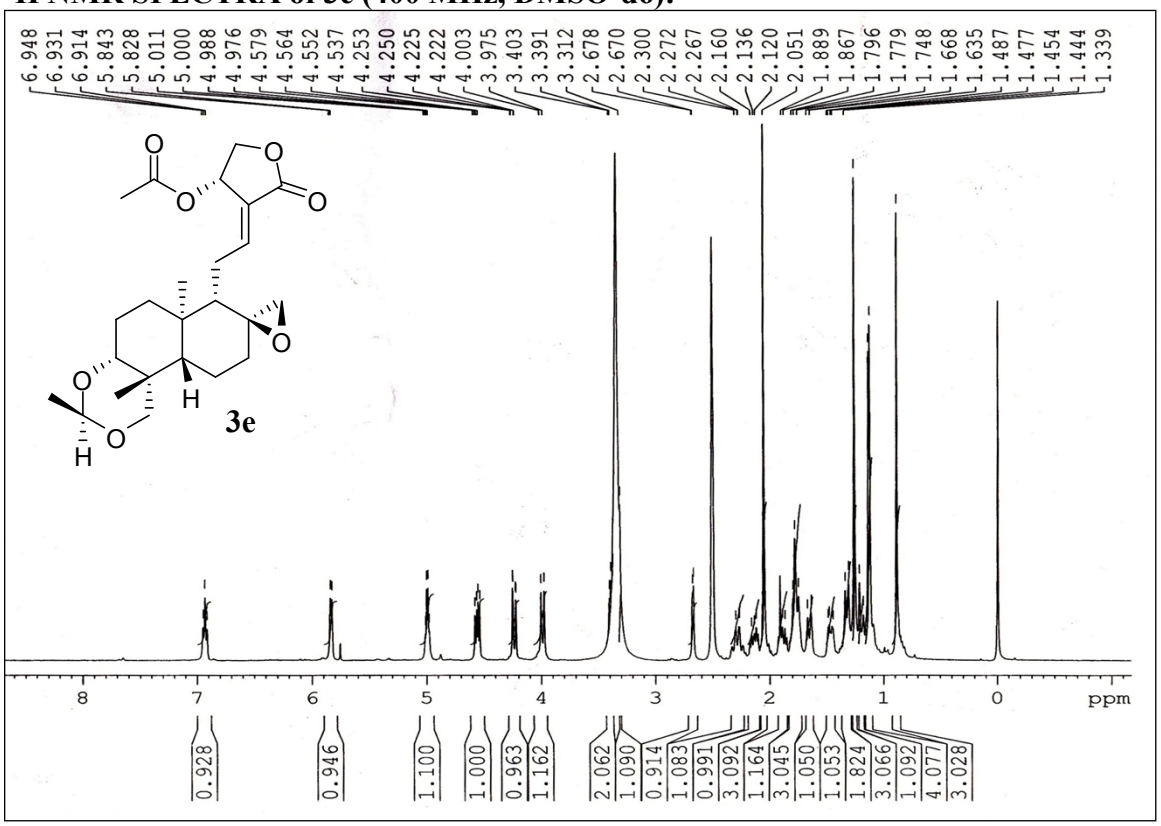

^{13}C NMR SPECTRA of 3e (125 MHz, DMSO-d6):

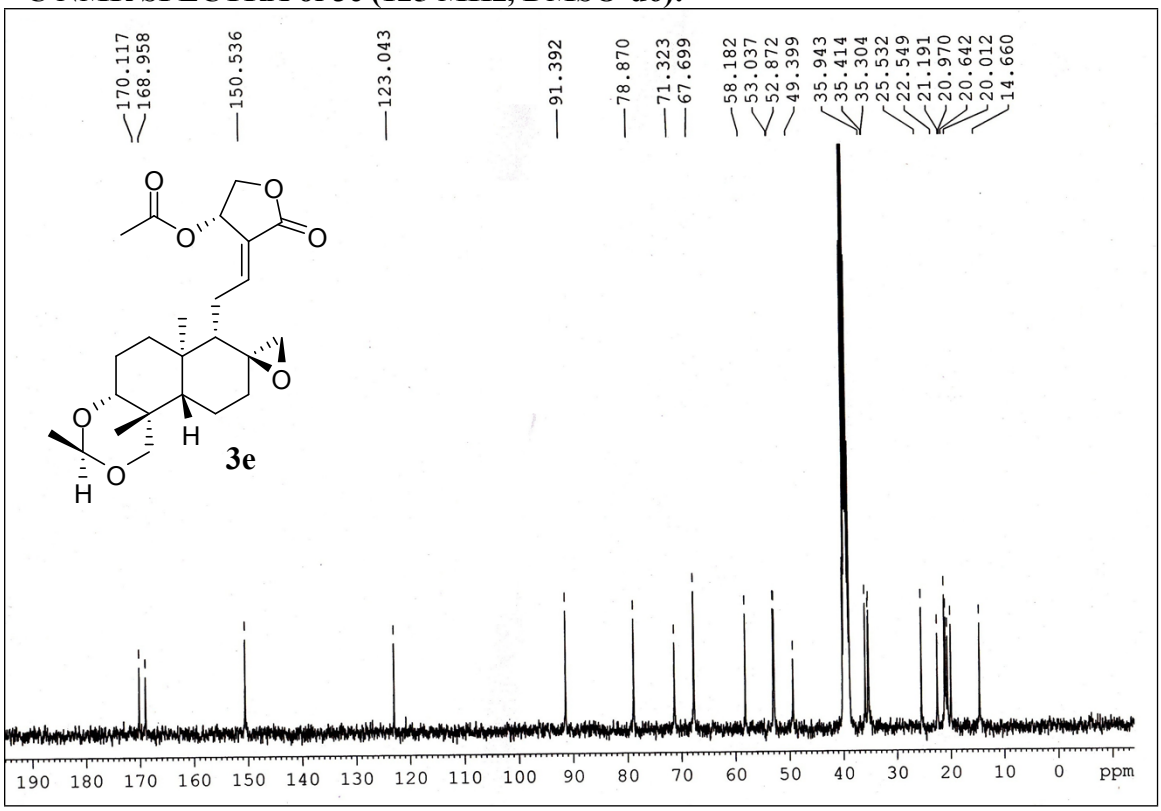

ESI-MASS SPECTRA of 3e:

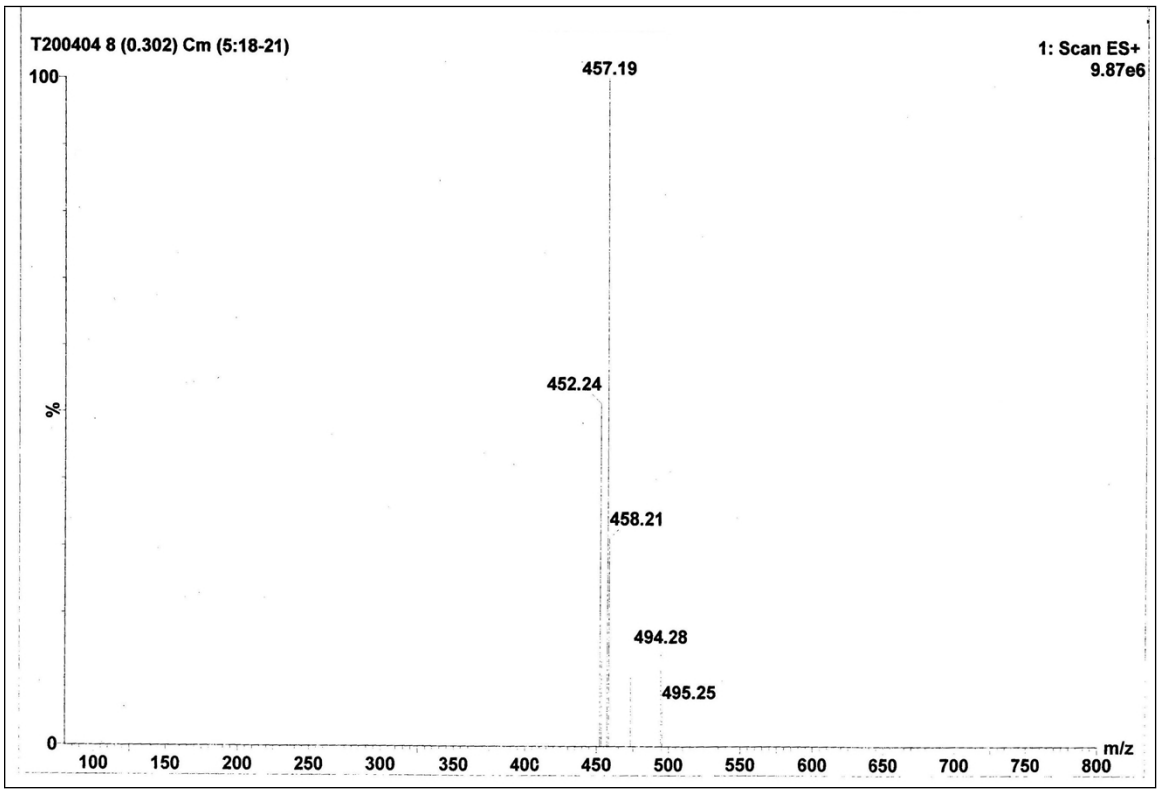

IR SPECTRA of 3e (KBr):

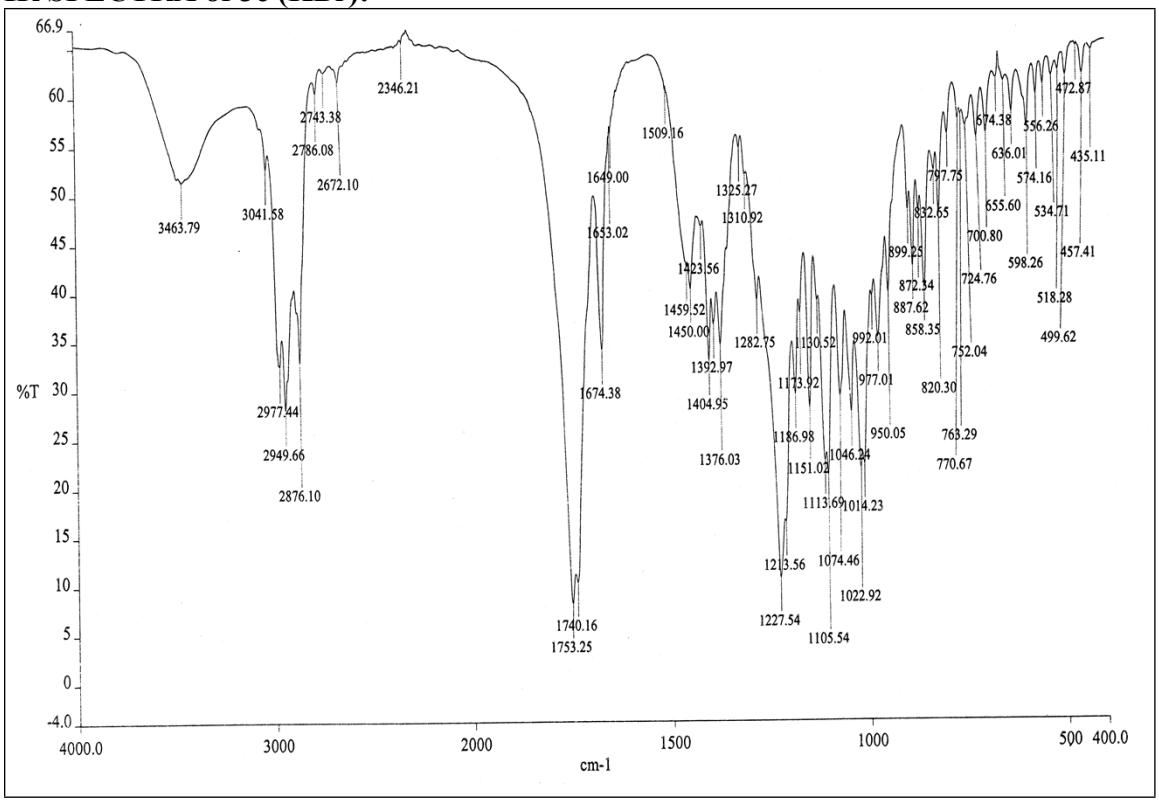

^{1}H NMR SPECTRA of 3f (300 MHz, $CDCl_3$):

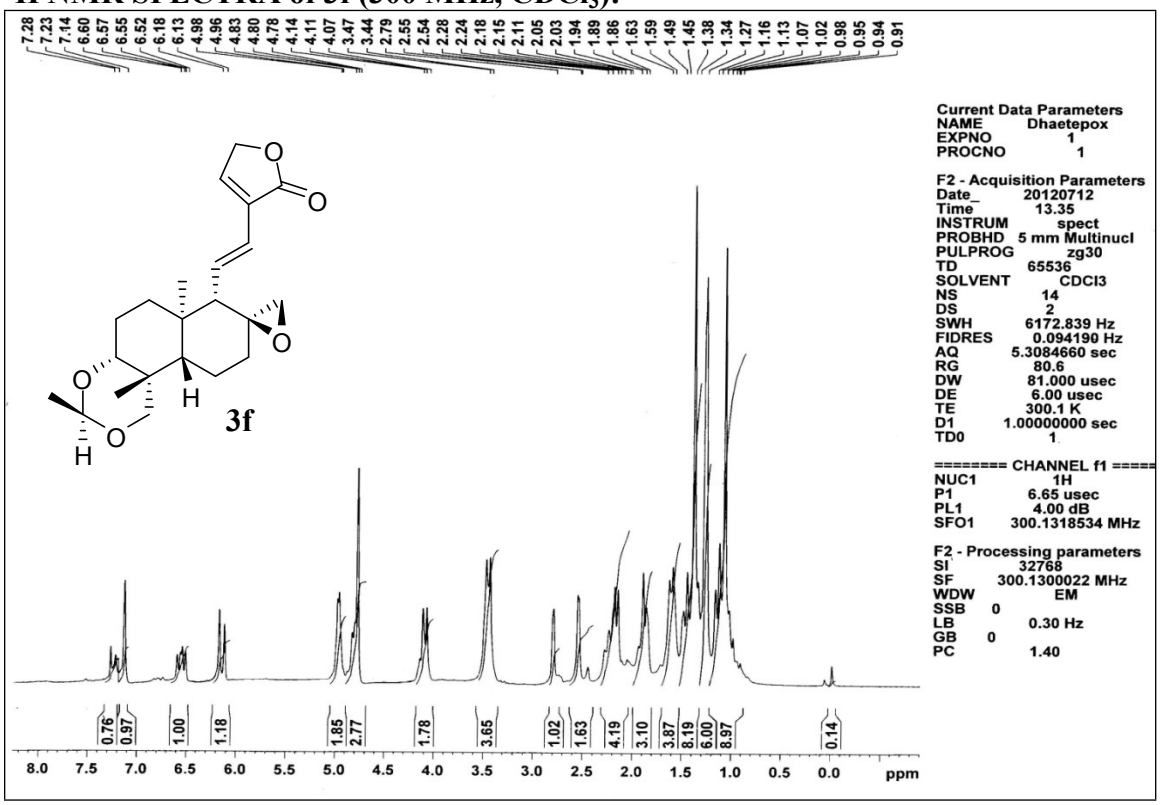

^{13}C NMR SPECTRA of 3f (75 MHz, $CDCl_3$):

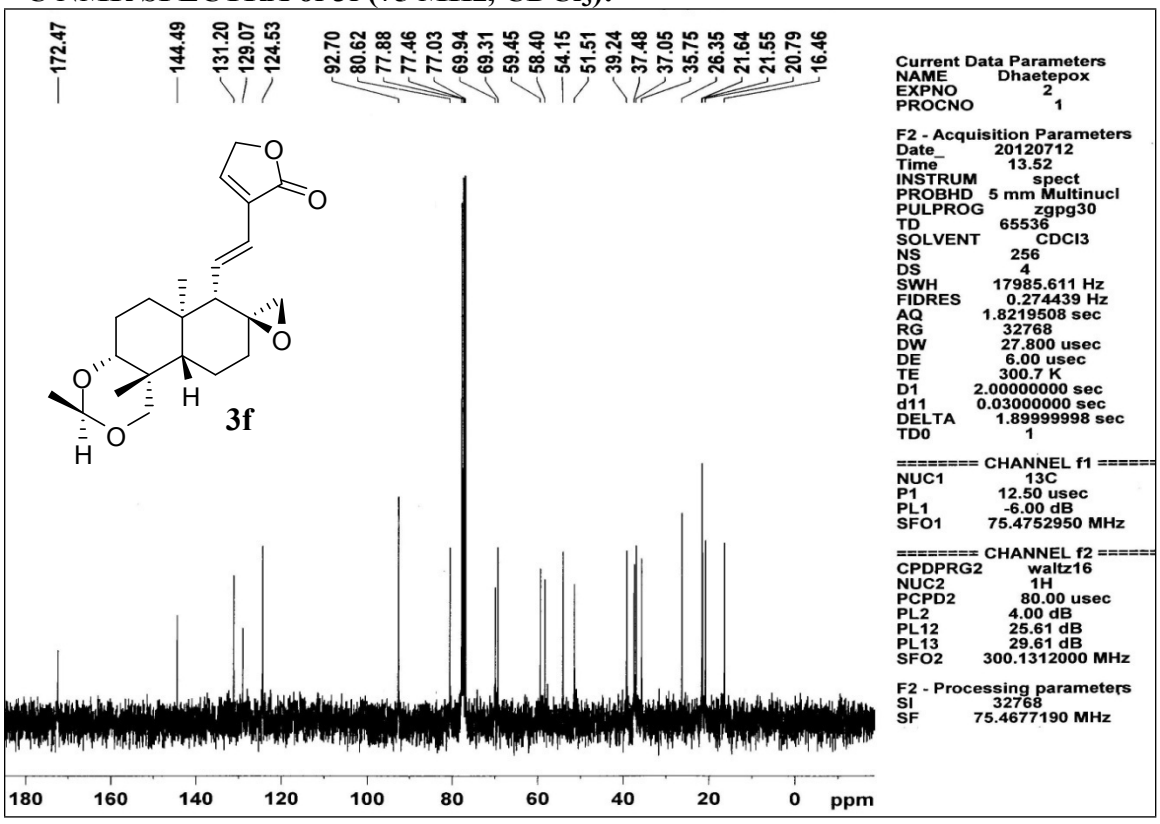

ESI-MASS SPECTRA of 3f:

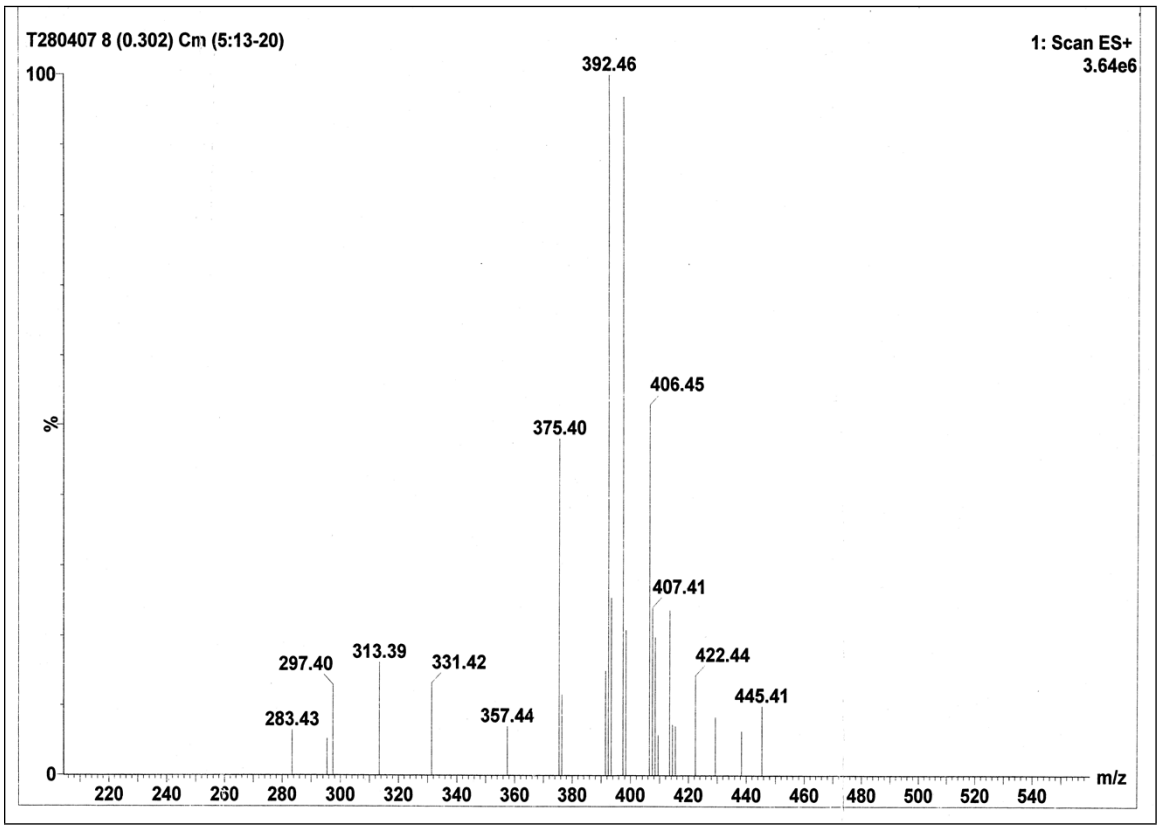

IR SPECTRA of 3f (KBr):